Purification and Characterization of the Human γ-Secretase Complex†

Patrick C. Fraering,‡ Wenjuan Ye,‡ Jean-Marc Strub,§ Georgia Dolios,|| Matthew J. LaVoie,‡ Beth L. Ostaszewski,‡ Alain van Dorsselaer,§ Rong Wang,|| Dennis J. Selkoe,*,‡ and Michael S. Wolfe*,‡

Center for Neurologic Diseases, Brigham and Women's Hospital and Harvard Medical School, Boston, Massachusetts 02115, Laboratoire de Spectrometrie de Masse Bio-Organique, ECPM, 25 rue Becquerel, 67087 Strasbourg cedex, France, and Department of Human Genetics, Mount Sinai School of Medicine, New York, New York 10029

Received March 12, 2004; Revised Manuscript Received May 12, 2004

ABSTRACT: γ-Secretase is a member of an unusual class of proteases with intramembrane catalytic sites. This enzyme cleaves many type I membrane proteins, including the amyloid β-protein (Aβ) precursor (APP) and the Notch receptor. Biochemical and genetic studies have identified four membrane proteins as components of γ-secretase: heterodimeric presenilin (PS) composed of its N- and C-terminal fragments (PS-NTF/CTF), a mature glycosylated form of nicastrin (NCT), Aph-1, and Pen-2. Recent data from studies in *Drosophila*, mammalian, and yeast cells suggest that PS, NCT, Aph-1, and Pen-2 are necessary and sufficient to reconstitute γ-secretase activity. However, many unresolved issues, in particular the possibility of other structural or regulatory components, would be resolved by actually purifying the enzyme. Here, we report a detailed, multistep purification procedure for active γ-secretase and an initial characterization of the purified protease. Extensive mass spectrometry of the purified proteins strongly suggests that PS-NTF/CTF, mNCT, Aph-1, and Pen-2 are the components of active γ-secretase. Using the purified γ-secretase, we describe factors that modulate the production of specific Aβ species: (1) phosphatidylcholine and sphingomyelin dramatically improve activity without changing cleavage specificity within an APP substrate; (2) increasing CHAPSO concentrations from 0.1 to 0.25% yields a ∼100% increase in Aβ42 production; (3) exposure of an APP-based recombinant substrate to 0.5% SDS modulates cleavage specificity from a disease-mimicking pattern (high Aβ42/43) to a physiological pattern (high Aβ40); and (4) sulindac sulfide directly and preferentially decreases Aβ42 cleavage within the purified complex. Taken together, our results define a procedure for purifying active γ-secretase and suggest that the lipid-mediated conformation of both enzyme and substrate regulate the production of the potentially neurotoxic Aβ42 and Aβ43 peptides.

A cardinal pathogenic feature of Alzheimer's disease (AD)[1] is the progressive accumulation of amyloid β-protein (Aβ) in brain regions subserving memory and cognition (*1*). Sequential proteolytic cleavages of the amyloid β-protein precursor (APP) by β-secretase and γ-secretase generate the amyloid β-proteins (Aβ) of 38−43 amino acids (*1*). β-Secretase (BACE) is a single membrane-spanning aspartyl protease expressed at high levels in neurons (*2*). γ-Secretase is also an aspartyl protease (*3*, *4*) but with a novel intramembranous catalytic site that is required for the cleavage of a wide range of type I membrane protein substrates that includes APP and the Notch receptors (*5*−*9*). In cells, γ-secretase activity is associated with a high molecular weight complex of integral membrane proteins that contains at least presenilin (PS) 1 or 2, nicastrin (NCT), Aph-1, and Pen-2 (*10*−*13*). Because of their respective roles in the generation of Aβ proteins, β- and γ-secretases have emerged as key therapeutic targets for AD (*14*).

Studies performed in *Drosophila* and mammalian cells have demonstrated that nicastrin, Aph-1, and Pen-2 stabilize and promote the increased formation of mature PS N- and C-terminal fragments and γ-secretase activity, suggesting that PS heterodimers, nicastrin, Aph-1, and Pen-2 are both necessary and sufficient for γ-secretase activity (*11*, *12*). The reconstitution of γ-secretase activity in *Saccharomyces cerevisiae*, which lacks this enzyme, by expressing these four components (*13*) strongly supports this conclusion.

Despite this progress, widely differing estimates of the size of the γ-secretase complex (*12*, *15*−*17*), the large diversity of its substrates (*18*−*23*), and the variability in cleavage site specificity (*18*−*23*) raise the question of whether other functional or regulatory components are associated with this

† This work was supported by the Swiss National Science Foundation (P.F., 81FR-68842), by CA88325 from the NCI and AG10491 from the NIA (R.W.), by the Alzheimer's Association and an NIH Training Grant (M.J.L), by AG15379 from the NIA and a Pioneer Award from the Alzheimer's Association (D.J.S), and by AG17574 from the NIA and IIRG-01-3078 from the Alzheimer's Association (M.S.W).

* To whom correspondence should be addressed. Tel: (617) 525-5511. Fax: (617) 525-5252. E-mail: (M.S.W.) mwolfe@rics.bwh.harvard.edu; (D.J.S.) dselkoe@rics.bwh.harvard.edu.

‡ Brigham and Women's Hospital and Harvard Medical School.

§ Laboratoire de Spectrometrie de Masse Bio-Organique.

|| Mount Sinai School of Medicine.

[1] Abbreviations: Aβ, amyloid-β protein; AD, Alzheimer's disease; APP, amyloid β-protein precursor; AICD, APP intracellular domain; CHO, Chinese hamster ovary; CTF, C-terminal fragment; ELISA, enzyme-linked immunosorbent assay; ER, endoplasmic reticulum; FAD, familial Alzheimer's disease; GST, glutathione-*S*-transferase; GSH, glutathione; HMW, high molecular weight; IP, immunoprecipitation; NCT, nicastrin; NTF, N-terminal fragment; PC, phosphatidylcholine; PE, phosphatidylethanolamine; PS, presenilin; SM, sphingomyelin; TM, transmembrane; TMD, transmembrane domain; WT, wild-type.

10.1021/bi0494976 CCC: $27.50
Published on Web 07/10/2004

enzyme. Moreover, rigorous biochemical characterization of the properties of this unusual enzyme requires fully purified γ-secretase. To assess these critical unanswered questions and define the details of the composition, mechanism, and structure of γ-secretase, we have developed a method for high-grade purification of the enzyme complex. Here, we report this procedure together with a detailed mass spectral analysis of all the proteins found in the catalytically active fraction recovered after the last step of the purification. This analysis strongly suggests that PS-NTF and -CTF, mNCT, Aph-1, and Pen-2 are sufficient for γ-secretase activity.

The most aggressive known forms of familial AD are caused by missense mutations in the genes encoding APP, PS1, and PS2. These mutant genes produce a common pathological phenotype of altered APP processing that elevates production of the strongly self-aggregating 42-residue form of Aβ (*24*−*28*). However, the biochemical mechanism by which presenilin/γ-secretase is modified to produce increased amounts of Aβ42 remains unclear. In an effort to identify and better understand factors (e.g., detergents, lipids, pH, inhibitors) that modulate the cleavage specificity of γ-secretase within the APP transmembrane (TM) domain, we characterized the activity of the complex following its purification.

EXPERIMENTAL PROCEDURES

Cell Lines and Cultures. Chinese hamster ovary (CHO) cell line γ-30 (expressing human PS1, Flag-Pen-2, and Aph1α2-HA) was cultured as previously described (*12*). The S-1 cell line (expressing human PS1, Flag-Pen-2, Aph1α2-HA, and NCT-GST) was cultured as previously described (*29*). In vitro γ-secretase assays using the recombinant APP-based substrate C100Flag and Aβ ELISAs were performed as previously described (*30*, *31*).

Multistep Purification of γ-Secretase from γ-30 Cells. (1) Cell Membrane Preparation. A total of 6.0×10^9 γ-30 cells were collected from 15 cm dishes and fully resuspended in 25 mL of MES buffer (50 mM MES, pH 6.0, 150 mM NaCl, 5 mM NaCl, 5 mM $CaCl_2$, plus complete protease inhibitor cocktail (Roche)). The cells were lysed by being passed once through a French press at greater than 1000 psi, and the nuclei and unbroken cells were harvested at 3000*g* for 10 min in a Sorvall SA600 rotor. The postnuclear supernatant was saved and centrifuged (100 000*g* for 1 h in a SW41 rotor) to pellet the total membranes (equals membrane preparation).

(2) Bicarbonate Wash. The membrane pellet was fully resuspended in 5 mL of ice-cold sodium bicarbonate buffer (0.1 M $NaHCO_3$, pH 11.3) by pipeting up and down at least 30 times, then incubated at 4 °C for 20 min. The washed membranes were then pelleted at 100 000*g* for 1 h at 4 °C.

(3 and 4) Complex Solubilization and Glycerol Velocity Gradient. The bicarbonate-washed membranes were fully resuspended in 5 mL of solubilization buffer (1% CHAPSO, 50 mM HEPES, pH 7.0, 150 mM NaCl, 5 mM $MgCl_2$, 5 mM $CaCl_2$) by being pipetted up and down at least 30 times. The membranes were then incubated at 4 °C for 1 h. To pellet the insoluble material, the solution was centrifuged (100 000*g* for 1 h), the pellet was discarded, and the supernatant was saved; this lysate is defined as solubilized γ-secretase preparation. The protein concentration was measured with the BCA reagent to be approximately 0.10 −0.25 mg/mL, and this solubilized γ-secretase preparation was freshly used to run the glycerol velocity gradient separation. The 18−28% gradients were prepared by layering 1 mL of each of the glycerol stock solutions (prepared in 0.2% digitonin-HEPES), from 28% on the bottom to 18% on the top. Then, 1 mL of the solubilized γ-secretase preparation was loaded onto the gradient and centrifuged at 200 000*g* for 15 h at 4 °C. A total of 12 fractions (1 mL per fraction) were collected from the bottom of the tubes after being punctured with a needle. The γ-secretase complex was detected in the gradient by analyzing each fraction by Western blotting for nicastrin (with R302 antibodies), PS1 holoprotein and -NTF (with Ab14), PS1-CTF (with 13A11), Flag-Pen-2 (with M2), and Aph1α2-HA (with 3F10). The fractions containing γ-secretase were pooled and defined as the glycerol gradient pooled fraction (23% of glycerol, 0.2% digitonin-HEPES).

(5) Affinity Chromatography with Immobilized Hydroxyethyl-Urea Transition State Analogue III-C. The glycerol gradient pool was diluted 1:2 in 1% CHAPSO-HEPES (7% glycerol, 0.66% CHAPSO, 0.066% digitonin-HEPES) and injected onto a III-^{31}C column (hydroxyethyl-urea transition state analogue inhibitor immobilized through its C-terminus to agarose beads via a six-atom hydrophilic linker (*31*)) installed into a Pharmacia AKTA-FPLC chromatography system by using a 50 mL superloop. After the column was washed in 1% CHAPSO-HEPES buffer, the bound protein was eluted in 1% Brij35-HEPES buffer. The eluted fractions enriched in γ-secretase were identified by Western blot as mentioned previously and pooled in one fraction defined as the III-^{31}C pooled fraction.

(6) Anti-Flag M2 Affinity Purification. The III-31C pool (1% Brij35-HEPES) was diluted 1:4 with 0.1% Digitonin-TBS buffer (0.1% digitonin, 50 mM tris HCl, 150 mM NaCl, pH 7.4) (final detergent concentration: 0.2% Brij35, 0.08% digitonin) and incubated overnight, in batch, with anti-Flag M2 affinity resin (Sigma) preequilibrated in 0.1% digitonin-TBS buffer. The beads were washed three times in the same buffer, and the bound proteins eluted with 0.2 mL of this buffer containing 200 μg/mL of Flag peptides (Sigma). This elution step was repeated three times, and the eluted fractions were pooled (M2 pooled fraction).

Multistep Purification of γ-Secretase from S-1 Cells. (1−*3) Cell Membrane Preparation, Bicarbonate Wash, and Complex Solubilization* were performed exactly as described previously for the γ-30 cells, except for the number of cells used in this procedure (2.5×10^9).

(4) GSH Affinity Purification. The solubilized γ-secretase preparation was diluted two times in HEPES buffer (final CHAPSO concentration = 0.5% corresponding to the optimal binding condition of active γ-secretase to the GSH beads, data not shown) and incubated overnight at 4 °C with gentle rocking with 2.5 mL of GSH resin (Amersham Biosciences, Sweden) preequilibrated in 0.5% CHAPSO-HEPES buffer. The resin was washed three times with 20 resin volumes of HEPES buffer (50 mM HEPES, pH 7.0, 150 mM NaCl) containing 0.5% CHAPSO. The bound proteins were eluted with one resin volume of elution buffer (0.5% CHAPSO-HEPES containing 25 mM of reduced GSH, pH 7.5).

(5) Anti-Flag M2 Affinity Purification. The proteins eluted from the GSH affinity resin were then diluted 6-fold in 0.1%

digitonin-HEPES (the optimal binding condition of active γ-secretase to the M2 resin, data not shown) and incubated overnight at 4 °C and with gentle rocking with 2.5 mL of anti-Flag M2 resin preequilibrated in 0.1% digitonin-TBS buffer. The resin was washed three times with 20 resin volumes of 0.1% digitonin-HEPES, and the bound proteins were released twice with one resin volume of M2 elution buffer defined in the γ-30 section stated previously.

(6) Hydroxyethyl-Urea Transition State Analogue ^{31}C Affinity Chromatography. The proteins eluted from the anti-Flag M2 affinity resin were diluted 1:2 in 1% CHAPSO-HEPES and incubated overnight at 4 °C with gentle rocking with 2.5 mL of III-31C affinity resin. The resin was washed three times with 20 resin volumes of 1% CHAPSO-HEPES, and the bound proteins were released with one resin volume of 1% Brij35-HEPES buffer (elution step repeated three times).

Tryptic Digestion and Mass Spectrometry. The fractions recovered after the last step of the purification procedures were concentrated by ultrafiltration (4 °C/7000 g/2 h) using a Microcon 3KD centrifugation device (Millipore, MA) and loaded onto a preparative SDS−PAGE (4−20%) gel. The gel was stained with silver nitrate (BioRad), and the visible bands were excised and cut into small pieces with a scalpel. The gel pieces were washed with 100 μL of 25 mM NH_4HCO_3, dehydrated twice with 100 μL of acetonitrile, and dried with a SpeedVac evaporator before reduction (10 mM DTT in 25 mM NH_4HCO_3) and alkylation (55 mM iodoacetamide in 25 mM NH_4HCO_3). For the tryptic digestion, the gel pieces were resuspended in three gel volumes of trypsin (12.5 ng/μL) freshly diluted in 25 mM NH_4HCO_3 and incubated overnight at 35 °C. The digested peptides were then extracted from the gel in a buffer containing 25% H_2O, 70% acetonitrile, and 5% HCOOH and analyzed by matrix-assisted laser desorption/ionization time-of-flight (MALDI-TOF) and LC/MS/MS. For nano-HPLC, a CapLC system (Micromass Ltd., Manchester, UK) was used. The samples were concentrated on a precolumn, and the peptides were separated on a 15 cm × 75 μm i.d. column packed with 3 μm 100 Å C18 PepMap (LC-Packings). The MS and MS/MS analyses were performed with a Q-TOF 2 hybrid quadrupole/time-of-flight mass spectrometer (Micromass Ltd., Manchester, UK) equipped with a Z-spray ion source. LC/MS/MS data were processed automatically with the ProteinLynx Process (Micromass) module. Data analysis was performed with Global Server (MicroMass, Ltd., Manchester, UK) software and Mascot (Matrix Science Ltd., London, UK) against NCBI (The National Center for Biotechnology Information) database.

Enzyme Kinetics and Data Analysis. In vitro γ-secretase assays were performed as previously described (*30*, *32*) except for samples in which no SDS was added to the C100Flag substrate preparations before the activity assays.

K_m and V_{max}. All the reactions contained C100Flag substrate at a defined concentration, purified γ-secretase solubilized in 0.25% CHAPSO-HEPES, pH 7.5, or 0.05% digitonin-HEPES, pH 7.5, at 10-fold dilution from stock (M2 anti-Flag eluted fraction, purification protocol from S-1 cells, step 5 in Figure 3A), 0.025% phosphatidylethanolamine (PE), and 0.10% phosphatidylcholine (PC).

pH Dependence of γ-Secretase Activity. Reactions were run with γ-secretase solubilized at 5-fold dilution from stock in defined buffers containing 0.25% CHAPSO or 0.05% digitonin. For pH 5.0−6.5, 50 mM MES was used, while 50 mM PIPES was used for pH 7.0−9.0.

Detergent Dependence of γ-Secretase Activity. Reactions were run with γ-secretase solubilized at 10-fold dilution from stock in defined buffers containing varying concentrations of CHAPSO (0.1−1% final concentration) or digitonin (0.01−1% final concentration).

Lipid Dependence of γ-Secretase Activity. Reactions were run with γ-secretase solubilized at 10-fold dilution from stock in 0.1% CHAPSO-HEPES, pH 7.5 containing various concentrations (0.0125−0.2% final concentration) of PC, PE, or sphingomyelin (SM). Cholesterol was solubilized in a mixture of 10 volumes of chloroform, 10 volumes of methanol, and 3 volumes of water (called 10:10:3) at a concentration of 25 mg/mL. A total of 1 μL of different cholesterol stock solutions (diluted in 10:10:3) was added to 5 μL of PC (10 mg/mL) + 2.5 μL of PE (5 mg/mL) + 5μL of SM (5 mg/mL; PC, PE, and SM all solubilized in 1% CHAPSO-HEPES, pH 7.5), thus yielding the so-called total lipid mixture (14 μL). The total lipid mixture was then added to the purified complex (50 μL) and assayed for C100Flag cleavage. The final CHAPSO concentration in these reactions was 0.25%.

γ-Secretase Inhibitors. DAPT, III-31C, and sulindac sulfide were added to the reactions from a DMSO stock (final DMSO concentration of 1%, which alone did not affect γ-secretase activity). All the reactions were stopped by adding 0.5% SDS, and the samples were assayed for Aβ40 and Aβ42 by ELISA as described (*33*). The capture antibodies were 2G3 (to Aβ residues 33−40) for the Aβ40 species and 21F12 (to Aβ residues 33−42) for the Aβ42 species.

Immunoprecipitation/Mass Spectrometry (IP/MS) Analysis of Aβ. Aβ peptides generated in the γ-secretase in vitro assays described previously were immunoprecipitated using monoclonal anti-Aβ antibody 4G8 (Senetek, Maryland Heights, MO) and protein A/G-plus agarose beads (Oncogene) and subjected to MALDI-TOF mass spectrometric analysis using a Voyager-DE STR mass spectrometer (Applied Biosystems) as described (*34*). The molecular masses were accurately measured and searched against the amino acid sequence of human APP C99 with addition of a methionine residue at the N-terminus and a Flag tag sequence at the C-terminus (C100Flag).

Western Blotting, Antibodies, and BN-PAGE. For Western analysis of PS1-NTF, PS1-CTF, Aph1α2, Pen-2, and NCT, the samples were run on 4−20% Tris-glycine PAGE gels, transferred to poly(vinylidene difluoride), and probed with Ab14 (for PS1-NTF, 1:2000, a gift of S. Gandy), N19 (for PS1-NTF, 1:200, Santa Cruz), 13A11 (for PS1-CTF, 5 mg/mL, a gift of Elan Pharmaceuticals), 3F10 (for Aph1α2-HA, 50 ng/mL, Roche), anti-Flag M2 (for Flag-Pen-2, 1:1000, Sigma), R302 (for NCT, 1:4000, a gift of D. Miller and P. Savam), guinea pig anti-NCT (1:2000, Chemicon), or αGST antibodies (for NCT-GST, 1:3000, Sigma). Samples from the γ-secretase activity assays were run on 4−20% Tris-glycine gels and transferred to poly(vinylidene difluoride) membranes to detect AICD-Flag or to nitrocellulose membranes to detect Aβ. The Flag-tagged substrate and AICD product generated by γ-secretase proteolysis were both detected with anti-Flag M2 antibodies; the other product, Met-Aβ, was detected with the anti-Aβ 6E10 antibody.

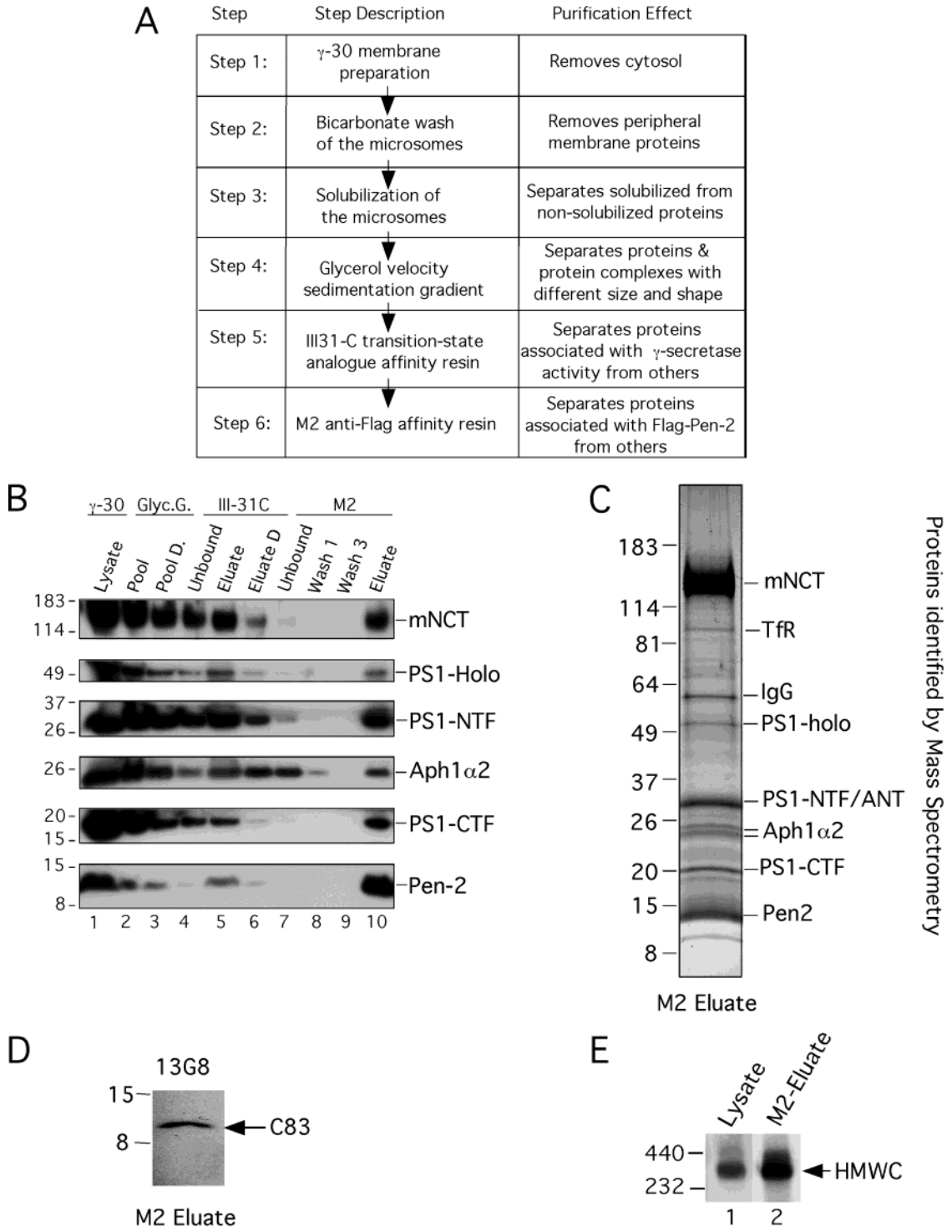

FIGURE 1: Purification of γ-secretase from γ-30 cells. (A) Scheme of γ-secretase purification protocol. CHO cells overexpressing human PS1, Aph-1-HA, and Flag-Pen-2 (γ-30 cell line) were used for a six-step purification procedure as outlined and as described in the text. (B) A total of 25 μL of each of the 1% CHAPSO-solubilized lysate (lysate, lane 1), the 0.2% digitonin glycerol gradient pooled fractions before (Glyc.G. pool, lane 2) and after dilution in 1% CHAPSO (Glyc.G. pool D, lane 3), the material not binding to the III-31C affinity column (III-31C unbound, lane 4), the 1% Brij35 III-31C eluate before (III-31C-eluate, lane 5) and after dilution in 0.1% digitonin (III-31C-eluate D, lane 6), the material not binding to the M2 affinity column (M2-Unbound, lane 7), the first and third washes (M2-Wash1 and M2-Wash3, lanes 8 and 9), and the fraction eluted from the M2 anti-Flag affinity resin (M2-Eluate, lane 10) were all loaded onto a 4−20% Tris-Glycine gel for SDS−PAGE. The presence of the γ-secretase components was confirmed by probing a Western blot with R302 (Nicastrin), Ab14 (PS1-holo and -NTF), 13A11 (PS1-CTF), 3F10 (Aph-1-HA), and M2 (Flag-Pen-2). (C) The proteins recovered after the last step of the purification procedure (M2-Eluate) derived from 3.0×10^9 of γ-30 cells were pooled, concentrated, separated on 4−20% Tris-Glycine by SDS−PAGE, and stained with silver nitrate. Each band visible on the gel was excised and subject to tryptic digestion; the peptides generated were separated and analyzed by LC/MS and LC/MS/MS. (D) C83 is labeled in the M2-eluted fraction by 13G8 and comigrates with the silver-positive 10 kDa band observed in Figure 1C. (E) BN-PAGE analysis of γ-secretase from γ-30 membranes solubilized in 1% Digitonin (lysate) and recovered after the last step of the purification procedure described in Figure 1A (M2 Eluate) confirms the integrity of the purified complex. Proteins were electrophoresed on 5−19.5% BN-PAGE gels and probed with Ab14, antibodies against N-terminal fragment of PS1.

NCT (Mus Musculus)

MATTRGGSGPDPGSRGLLLLSFSVVLAGLCGGNSVERKIYIPLNKTAPCVRLLNATHQIGCQSSISGDTGVIHVVEKEED 80
LKWVLTDGPNPPYMVLLEGKLFTRDVMEKLKGTTSRIAGLAVTLAKPNSTSSFSPSVQCPNDGFGIYSNSYGPEFAHCKK160
TLWNELGNGLAYEDFSFPIFLLEDENETKVIKQCYQDHNLGQNGSAPSFPLCAMQLFSHMHAVISTATCMRRSFIQSTFS240
INPEIVCDPLSDYNVWSMLKPINTSVGLEPDVRVVVAATRLDSRSFFWNVAPGAESAVASFVTQLAAAEALHKAPDVTTL320
SRNVMFVFFQGETFDYIGSSRMVYDMENGKFPVRLENIDSFVELGQVALRTSLDLWMHTDPMSQKNESVKNQVEDLLATL400
EKSGAGVPEVVLRRLAQSQALPPSSLQRFLRARNISGVVLADHSGSFHNRYYQSIYDTAENINVTYPEWQSPEEDLNFVT480
DTAKALANVATVLARALYELAGGTNFSSSIQADPQTVTRLLYGFLVKANNSWFQSILKHDLRSYLDDRPLQHYIAVSSPT560
NTTYVVQYALANLTGKATNLTREQCQDPSKVPNESKDLYEYSWVQGPWNSNRTERLPQCVRSTVRLARALSPAFELSQWS640
STEYSTWAESRWKDIQARIFLIASKELEFITLIVGFSILIFSLIVTYCINAKADVLFVAPREPGAVSY 708

Sequence coverage : 12%
RMS Error : 20 ppm
Mascot score : 316

Human Pen-2

MNLERVSNEEKLNLCRKYYLGGFAFLPFLWLVNIFWFFREAFLVPAYTEQSQIKGYVWRSAVGFLFWVIVLTSWITIFQI 80
YRPRWGALGDYLSFTIPLGTP 102

Sequence coverage : 31%
RMS Error: 28 ppm
Mascot score : 59

Human Aph1α2

MGAAVFFGCTFVAFGPAFALFLITVAGDPLRVIILVAGAFFWLVSLLLASVVWFILVHVTDRSDARLQYGLLIFGAAVSV 80
LLQEVFRFAYYKLLKKADEGLASLSEDGRSPISIRQMAYVSGLSFGIISGVFSVINILADALGPGVVGIHGDSPYYFLTS160
AFLTAAIILLHTFWGVVFFDACERRRYWALGLVVGSHLLTSGLTFLNPWYEASLLPIYAVTVSMGLWAFITAGGSLRSIQ240
RSLLCRRQEDSRVMVYSALRIPPED 266

Sequence coverage : 13%
RMS Error : 23 ppm
Mascot score : 102

Human PS1

MTELPAPLSYFQNAQMSEDNHLSNTVRSQNDNRERQEHNDRRSLGHPEPLSNGRPQGNSRQVVEQDEEEDEELTLKYGAK 80
HVIMLFVPVTLCMVVVVATIKSVSFYTRKDGQLIYTPFTEDTETVGQRALHSILNAAIMISVIVVMTILLVVLYKYRCYK160
VIHAWLIISSLLLLFFFSFIYLGEVFKTYNVAVDYITVALLIWNFGVVGMISIHWKGPLRLQQAYLIMISALMALVFIKY240
LPEWTAWLILAVISVYDLVAVLCPKGPLRMLVETAQERNETLFPALIYSSTMVWLVNMAEGDPEAQRRVSKNSKYNAEST320
ERESQDTVAENDDGGFSEEWEAQRDSHLGPHRSTPESRAAVQELSSSILAGEDPEERGVKLGLGDFIFYSVLVGKASATA400
SGDWNTTIACFVAILIGLCLTLLLLAIFKKALPALPISITFGLVFYFATDYLVQPFMDQLAFHQFYI 468

Sequence coverage : 23%
RMS Error: 24 ppm
Mascot score : 388

FIGURE 2: Mass spectral identification of γ-secretase-associated proteins. Nicastrin (NCBI accession number 11037796), PS1-NTF, PS1-CTF (4506163), Aph1 (7705787), and Pen-2 (28144920) are the predominant proteins detected on the gel stained with silver nitrate (Figure 1C). Note that all the peptides identified by mass spectrometry (in red) are located outside of the predicted TMDs (in blue and underlined), except for two of them, which are in TMDs 5 and 7 of PS1. The trypsin proteolytic cleavage sites are in bold, whereas the presenilinase PS1 cleavage site is green. The mass spectrometric parameters (% of the sequence coverage, RMS error, and the Mascot score (http://www.matrixscience.com/ search_form_select.html)) are summarized for each protein.

Blue native gel electrophoresis was performed as previously described (*35*).

RESULTS

Purification and Identification of γ-Secretase Associated Proteins. Purification of Active γ-Secretase. We undertook a systematic evaluation of several possible purification steps and arrived at a protocol that involves six sequential steps (Figure 1A). We began with homogenization of large amounts of γ-30 cells, CHO cells stably overexpressing together human PS1, Aph1α2-HA, and Flag-Pen-2, which are characterized by a marked increase in γ-secretase activity (*12*). As a first purification step, total cellular membranes were prepared by differential centrifugation to largely remove cytosolic proteins. We have found that γ-secretase activity is still present in cell membrane prepara-

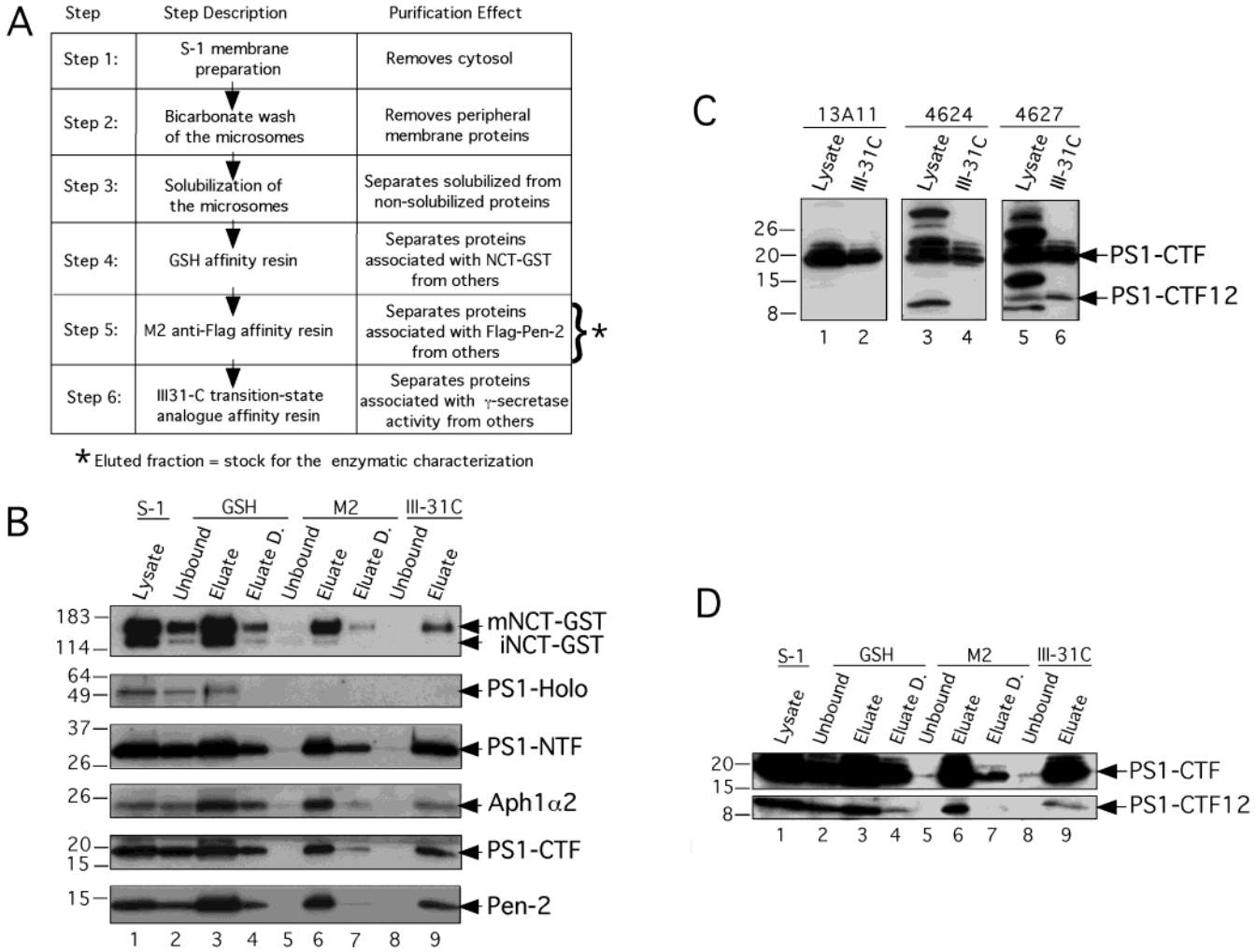

FIGURE 3: Purification of γ-secretase from S-1 cells reveals a 12 kDa fragment of the C-terminal PS1-CTF that copurifies with the complex. (A) Scheme of alternative γ-secretase purification protocol from S-1 cells. (B) A total of 25 μL of each of the 1% CHAPSO-solubilized lysate (S-1 lysate, lane 1), the material not binding to the GSH affinity resin (GSH-Unbound, lane 2), the fraction eluted from the GSH-affinity resin before (GSH-Eluate, lane 3) and after dilution in 0.1% digitonin (GSH-Eluate D., lane 4), the material not binding to the M2 anti-Flag affinity resin (M2-Unbound, lane 5), the fraction eluted from the M2 anti-Flag affinity resin before (M2-Eluate, lane 6) and after dilution in 1% CHAPSO (M2-Eluate D., lane 7), the material not binding to the III-31C affinity resin (31C-Unbound, lane 8), and the fraction eluted from the III-31C resin (31C-Eluate, lane 9) were all loaded onto a 4−20% Tris-Glycine gel for SDS−PAGE, and the presence of the γ-secretase components was confirmed by probing a Western blot as described (Figure 1B), except for NCT-GST, which was detected with anti-GST antibodies. (C) A 12 kDa fragment (PS1-CTF12) immunoreactive with 4627 (to PS1-CTF, residues 457−467), but not with 13A11 or 4624 (to PS1-CTF, residues 294−309 and 343−357, respectively) was detected in the final eluate after III-31C affinity purification (step 6 in Figure 3A). The high and low MW bands detected in the lysate with 4624 and 4627 antisera (lanes 3 and 5) but not with the affinity purified monoclonal antibody 13A11 (lane 1) suggest that these bands are nonspecific. (D) PS1-CTF12 remains associated with γ-secretase during purification. A total of 25 μL of the fractions recovered after each purification step (Figure 3B) was loaded onto a 4−20% Tris-Glycine gel, and PS1-CTF12 was detected with 4627.

tions after washing with bicarbonate buffer (0.1 M $NaHCO_3$, pH 11.3) (*31*). Such washing conditions remove residual cytosolic proteins and strip away almost all peripheral membrane proteins (*36*), leaving only integral or tightly associated membrane proteins. On the basis of these observations, we used bicarbonate wash of membrane preparations as a second purification step. These washed microsomes were then solubilized in a buffer containing 1% CHAPSO that allows all γ-secretase components to remain associated and in an active conformation (*32*); this was spun at 100 000*g* for 1 h, and the pellet was discarded (purification step 3). The next step (step 4) was a glycerol velocity sedimentation gradient in 0.2% digitonin, a purification step based on the size and shape of the complex (*37*, *38*). We previously found that γ-secretase components (γ-30 cell membranes solubilized in 1% digitonin) were all present in the same gradient fractions (20−23% glycerol), maintained their physical association, and contained proteolytic activity (*12*). Those fractions were pooled and injected over a III-31C affinity column for a separation based on binding of active γ-secretase (step 5). The III-31C affinity resin, a hydroxyethyl-urea transition state analogue inhibitor immobilized through its C-terminus to agarose beads via a six-atom hydrophilic linker, was developed to isolate functional γ-secretase activity (*31*). The bound proteins were eluted with 1% Brij35, and fractions enriched in γ-secretase were pooled and adjusted by dilution with 0.1% digitonin. As a last step of purification (step 6), we developed an M2 anti-Flag antibody immunoaffinity procedure, a separation based on the presence of Flag-Pen-2 in the active complex. The fractions eluted from the III-31C were diluted in 0.1% digitonin (optimal buffer condition for maximal binding to the resin; data not shown)

and incubated in batch mode with M2 anti-Flag affinity resin (Sigma), and the bound proteins were eluted with Flag peptides (200 μg/mL). All γ-secretase components were followed during the purification procedure by probing the fractions recovered after each step by Western blot (Figure 1B). The integrity of the purified complex was confirmed by Blue Native gel electrophoresis (Figure 1E) and by measuring γ-secretase activity with C100Flag substrate (data not shown). The proteins recovered after the last step of the purification procedure were concentrated by ultrafiltration, loaded onto a preparative SDS−PAGE (4−20%) gel, and stained with silver nitrate (Figure 1C). All visible bands were excised and analyzed by tryptic digestion and LC/MS + LC/MS/MS mass spectrometry.

Mass Spectral Identification of γ-Secretase Associated Proteins. As shown in Figure 1C, mNCT, PS1-NTF and -CTF, Aph-1, and Pen-2 are the predominant proteins identified by this procedure (tryptic peptides and corresponding masses available in Supporting Information Figure 1). Interestingly, almost all of the peptides identified by mass spectrometry after the tryptic digestion of NCT, PS1-NTF and -CTF, Aph-1, and Pen-2 are predicted to be hydrophilic; intramembranous peptides were not identified by mass spectrometry (Figure 2). PS1-holoprotein was also found in the purified γ-secretase preparation but in much smaller amounts than PS1-NTF, as suggested by the silver intensity of the two corresponding bands (holo, see Figure 1C). In addition, two extra proteins that were both visible on the silver-stained gel (Figure 1C) have also been identified by this procedure as transferrin receptor (TfR, 4507457) and IgG (21304449). ADP/ATP translocase (ANT, 399012) has also been identified in the 30 kDa band corresponding to PSN1-NTF. Both NTF and CTF of PS2 (NCBI accession number 14714537) were also detectable by this procedure and comigrated in the PS1-NTF and PS1-CTF bands. The analysis by tryptic digestion and LC/MS + LC/MS/MS of the total proteins contained in the purified fraction (to identify proteins that were not seen on the silver stained gel) also revealed a choline transporter (CD92, 16945323), prohibitin (1673514), and PS1-isoform 374 (7549815) produced by an alternative splicing that results in a frame shift with a stop codon, generating a truncated presenilin consisting of 374 amino acids (*39*). The amounts of tryptic fragments obtained from these three proteins were far less than those obtained from the four known γ-secretase components. The peptide sequence -TLLQRMMMAGSVR- (corresponding to residues 353−365 of the C-terminal domain of the PS1-374 isoform) was detected by LC-MS-MS. Because this peptide is not present in any other known form of PS1, we conclude that PS1-374 was specifically identified in the purified fraction. All proteins identified by both procedures are summarized in Table 1. Importantly, we were unable to coimmunoprecipitate ANT, CD92, prohibitin, PS1-isoform 374, or TfR with PS1-NTF (using X81 antibody to residues 1−81 of PS1-NTF) in a 1% CHAPSO-solubilized CHOwt lysate, and in turn, none of the four endogenous γ-secretase components were coprecipitated with these proteins, suggesting that they do not interact specifically with γ-secretase. Of note, the parental CHO line from which the γ-30 cells were prepared stably overexpresses TfR.

As shown in Figure 1C, a band corresponding to a ~10 kDa protein that we were not able to identify by mass spectrometry was detected on the silver stained SDS gel. Because we previously reported that C83, the major endogenous APP substrate of γ-secretase, is quantitatively associated with the endogenous complex in HeLa cells (*31*), we probed the purified fraction for C83 with 13G8, an antibody raised against residues 732−751 of APP751 (that also detects C99). Consistent with the apparent molecular weight of C83, a 10 kDa band was specifically labeled by 13G8, and it comigrated with the silver-positive 10 kDa band (Figure 1D), indicating that a small portion of C83 was also present in the purified fraction.

Table 1: Proteins Identified by Mass Spectrometry in the Fractions Recovered after the Last Step of the Purification Procedure Described in Figures 1A and 3A[a]

protein	NCBI number	MW (kDa)	cellular localization	function
nicastrin	24638433	78	PM, ER, G	protease
PS1-467	4506163	52	PM, ER, G	protease
Aph1	7705787	26	PM, ER, G	protease
Pen-2	28144920	12	PM, ER, G	protease
PS2	14714537	50	PM, ER, G	protease
ANT 3	399012	33	mitochondria	ADP/ATP carrier protein
PS1-374	7549815	42	PM, ER, G?	protease
CD92	16945323	73	PM, ER, G?	choline transport
prohibitin	1673514	30	mitochondria PM	cell cycle regulation chaperone
TfR	4507457	80	PM	iron transport

[a] The proteins confirmed as associated with γ-secretase are in bold. The γ-secretase associated candidates are in italics. The National Center for Biotechnology Information accession numbers are given. PM, plasma membrane; ER, endoplasmic reticulum; G, Golgi; and MW, molecular weight.

On the basis of the mass spectral identification of all γ-secretase associated proteins as well as on our coimmunoprecipitation results suggesting that neither ANT, CD92, prohibitin, PS1-isoform 374, nor TfR interact specifically with γ-secretase, our results strongly suggest that PS1-NTF, PS1-CTF, Aph1, mNCT, and Pen-2 are the essential components of purified γ-secretase. The latter observation is fully consistent with several recent reports (*11*−*13*) and represents the first definition of the components of γ-secretase by biochemical purification.

Characterization of the Purified γ-Secretase. We have previously found that 1% Brij35 is incompatible with the C100Flag in vitro γ-secretase activity assay: γ-secretase activity could be recovered from the Brij35 eluate off a preparative III-31C inhibitor column only after coimmunoprecipitation and a switch into optimal detergent (*31*), suggesting that removal of Brij35 allows subsequent change to an active protease conformation. In agreement with these observations, we found that (a) γ-secretase activity was recovered from the Brij35 eluate (Figure 1A, step 5) after coimmunoprecipitation and a switch into an appropriate buffer (0.2% CHAPSO-HEPES, pH 7.0) and (b) γ-secretase activity was recovered after the buffer exchange (from 1% Brij35 to 0.1% Digitonin) that occurred during the M2 anti-Flag affinity resin purification step (Figure 1A, step 6). However, the activity recovered after the III-31C affinity purification step (estimated from 50 μL of the fraction analyzed in lane 5, Figure 1B) was significantly lower than the activity recovered after the glycerol gradient purification step (estimated from 50 μL of the fraction analyzed in lane 3, Figure 1B), whereas similar amounts of γ-components

can be observed in these corresponding fractions (compare lanes 3 and 5, Figure 1B). These observations suggest only a partial recovery of activity after the III-31C affinity purification step and the buffer exchange promoted by the M2 anti-Flag affinity purification step (Figure 1A, step 6). To improve the recovery of active γ-secretase, we modified the purification protocol described previously (Figure 1A). We engineered a GST-tag on the C-terminus of NCT and stably transfected the γ-30 cell line, yielding the S-1 cell line, which has 2-fold higher γ-secretase activity than in the parental γ-30 line (*29*). On the basis of the purification protocol performed in γ-30 cells, we altered the order of the steps and added a GSH-based affinity purification step, yielding a modified protocol that involves six sequential steps (Figure 3A). In essence, the glycerol gradient step (Figure 1A, step 4) was replaced by the GSH-based affinity purification step (Figure 3A, step 4), and the III-31C affinity purification step was shifted to the last step. This modified procedure allows recovery of purified γ-secretase with improved activity eluted from the M2 anti-Flag affinity resin (Figure 3A, step 5) and provides a potent affinity method (III-31C resin, Figure 3A, step 6) useful for further purification and characterization of γ-secretase associated proteins.

All γ-secretase components were followed during the purification procedure by probing the fractions recovered after each step by Western blot (Figure 3B). The results confirmed that all γ-secretase components were present after the last purification step (III-31C chromatography). They also show that mNCT-GST (176 kDa) was enriched during the purification procedure (Figure 3B, lanes 6 and 9), supporting several reports that only mNCT is associated with the active γ-secretase complex (*40*−*42*). Next, the functional integrity and the purity of the complex recovered after the M2 anti-Flag affinity purification step (Figure 3A, step 5) were extensively checked in our C100Flag in vitro γ-secretase activity assay (see Figures 4−8) and by the mass spectral identification of the proteins recovered in the corresponding fraction (Supporting Information Figure 2). The protein profile obtained by silver staining of SDS gels is very similar to that observed after the last step in the γ-30 purification procedure (compare Figure 1C and Supporting Information Figure 2). On the basis of its relative purity and activity, the γ-secretase eluted from the M2 anti-Flag affinity resin was therefore used as stock for all subsequent in vitro reactions performed in the detailed enzymatic characterization described next. We should point out that we attempted to determine the enzymatic enrichment and yield in γ-secretase after each purification step; however, such determinations would not reflect the actual specific activities for two reasons. First, the specific elution of γ-secretase from both the GSH affinity resin and M2 anti-Flag affinity resin (using GSH and Flag peptides, respectively) leads to underestimation of the enrichment by virtue of overestimating the amount of recovered protein. Second, the purification protocol changes detergents between CHAPSO and digitonin to optimize the binding of the enzyme to the corresponding resins, but γ-secretase does not show the same activity in these different buffer conditions (*29*), thus making it impossible to quantitatively compare the activities recovered after each purification step. Nevertheless, the specific activities measured in the starting material (step 3, Figure 3A, which has already been purified in the sense that it contains only integral membrane proteins and overexpressed γ-components) and in the fractions eluted from the M2-anti Flag affinity resin (step 5, Figure 3A) were 0.2 pmol of Aβ40/min/mg of protein and 32 pmol of Aβ40/min/mg of protein, respectively; the corresponding enrichment was ∼160-fold, and the final yield was ∼22%.

A 12 kDa Fragment of the PS1-CTF Copurifies with γ-Secretase. We probed the III-31C eluted fraction recovered as the last purificaton step (step 6, Figure 3A) with 13A11, 4624, and 4627, antibodies raised against the N-terminal (13A11, to residues 294−309 and 4624, to residues 343−357) or C-terminal (4627, to residues 457−467) regions of the PS1-CTF fragment (Figure 3C, lanes 1−6). We found that 4627 is able to detect in this fraction a 12 kDa fragment (called here PS1-CTF12) that is minor when compared to PS1-CTF. 13A11 and 4624 were not able to detect PS1-CTF12 (Figure 3C, lanes 2 and 4), suggesting that this fragment is an N-terminally truncated PS1-CTF. The size of PS1-CTF12 is in good agreement with a caspase-3-mediated PS1-CTF fragment (∼14 kDa) reported to be generated during apoptosis by cleavage at D345 or S346 of PS1 (*43*, *44*). We also probed each fraction recovered during the purification procedure for PS1-CTF12 using the 4627 antibody and found that it copurifies with PS1-CTF (Figure 3D), suggesting that this fragment is present in at least a portion of the purified γ-secretase complexes (but very small when compared to PS1-CTF). No corresponding caspase-cleaved PS1-NTF fragments (*44*) were detected when probed with anti-PS1-NTF antibodies (Ab14), even at high exposures (data not shown).

Lipid Dependence of Aβ40 and Aβ42 Formation by Purified γ-Secretase. Biochemical studies of autopsied brain tissue from Alzheimer's disease patients have revealed reduced levels of a major membrane phospholipid, phosphatidylcholine (PC (*45*)). A decrease in membrane PC content has also been shown to cause cell death by apoptosis and cause increased cellular concentrations of ceramide, a putative second messenger of apoptosis and a precursor and a metabolite of sphingomyelin (SM), another membrane phospholipid (*46*). Moreover, we and others have demonstrated that PC and phosphatidylethanolamine (PE) are necessary to recover or improve in vitro γ-secretase activity (*30*, *47*). In light of these observations and to optimize in vitro γ-secretase activity obtained with the purified enzyme, we assessed the effect of various concentrations of PC, PE, and SM on both cleavage efficiency and cleavage specificity of C100Flag substrate incubated with purified γ-secretase (from step 5 in Figure 3A). The C100Flag substrate used in this study is a recombinant protein consisting of the β-CTF (C99) portion of APP (amino acids 596−695) plus a methionine (M) and a Flag tag at the N- and C-termini, respectively (*31*, *32*). The cleavage products, M-Aβ40 and M-Aβ42 (which we designate Aβ40 and Aβ42 for simplicity), were quantified by ELISA. We found that between 0.0125 and 0.1% of PC and SM each augmented Aβ40 production, whereas PE had very little or no effect in the same concentration range (Figure 4A). A higher concentration of these lipids (0.2%) did not increase (PC) or actually lowered (SM) Aβ40 production. Next, we assessed the effect of various concentrations of PC, PE, and SM on the cleavage specificity within the C100Flag substrate by quantifying both Aβ40 and Aβ42 by ELISA and found that increased

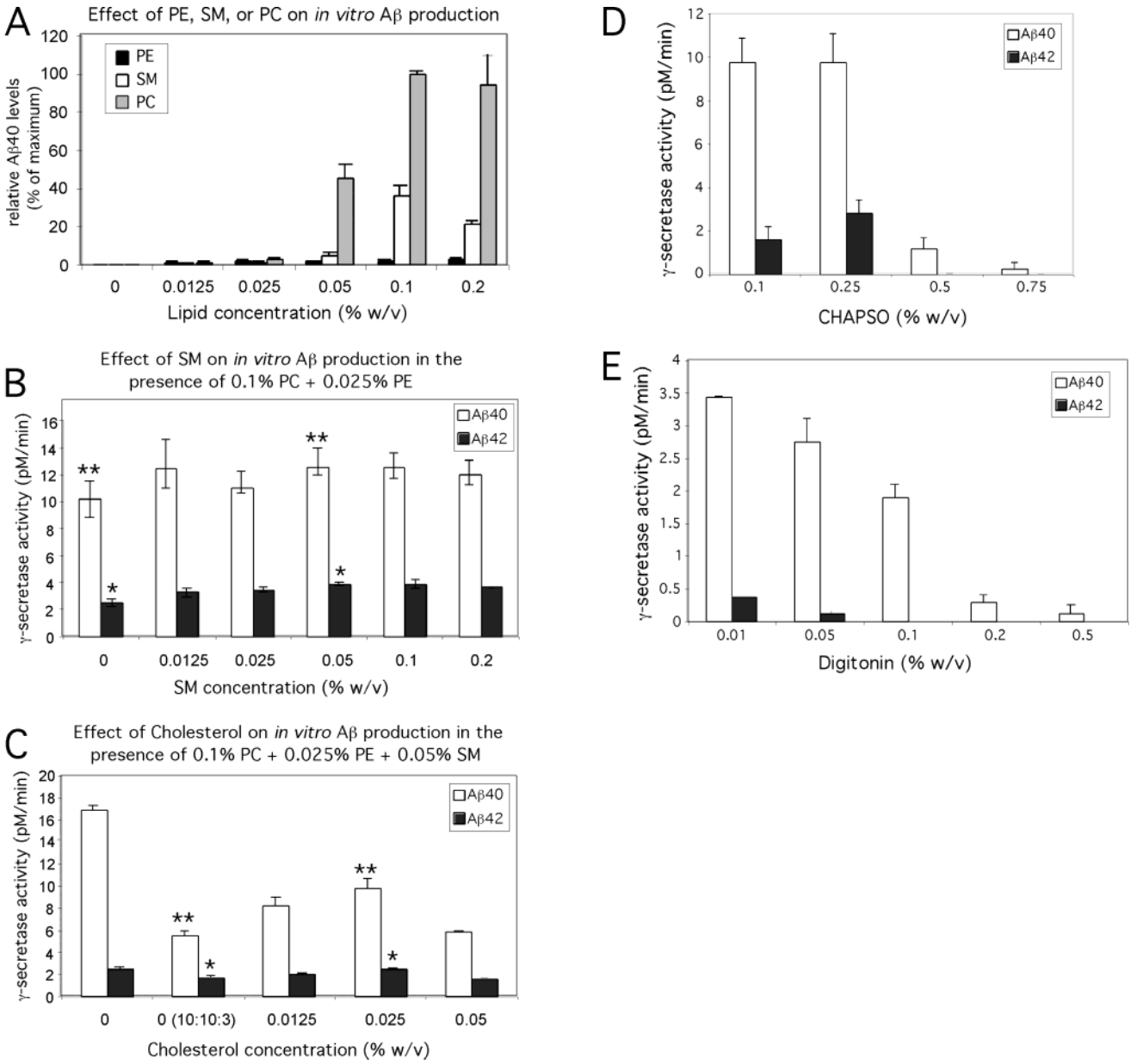

FIGURE 4: Effects of cell membrane lipids and detergents on the cleavage efficiency of C100Flag substrate by purified γ-secretase. (A) Effect of various concentrations of phosphatidylcholine (PC), phosphatidylethanolamine (PE), and sphingomyelin (SM) on the cleavage efficiency of the C100Flag substrate. The maximum activity occurred in 0.1% PC ($n = 3$). (B) Effect of various concentrations of SM on in vitro Aβ generation in the presence of 0.1% PC + 0.025% PE. The maximal potentiation by SM for both Aβ40 and Aβ42 production occurred in 0.05% SM. The asterisks indicate significant differences in the Aβ40 (**) and Aβ42 (*) production as compared to the samples without SM ($n = 2$; *, $p < 0.01$; **, $p < 0.0001$). (C) Effect of various concentrations of cholesterol on in vitro Aβ generation in the presence of 0.1% PC + 0.025% PE + 0.05% SM. The asterisks indicate significant differences in the Aβ40 (**) and Aβ42 (*) production relative to the samples without cholesterol ($n = 2$; *, $p < 0.001$; **, $p < 0.01$). Note that the solvent (a mixture of chloroform, methanol, and water in a 10:10:3 vol/vol ratio) used to solubilize cholesterol affects γ-secretase activity and more specifically the Aβ40 production. The final concentration of the solvent was the same for all cholesterol concentrations. (D) Detergent dependence of Aβ formation by purified γ-secretase diluted in buffers containing 0.1−0.75% CHAPSO-HEPES pH 7.5 ($n = 3$). (E) Detergent dependence of Aβ formation by purified γ-secretase diluted in buffers containing 0.01−0.5% digitonin-HEPES, pH 7.5. For the detergent dependence experiments, reactions were incubated at 37 °C for 180 min in 0.1% (w/v) PC, 0.025% (w/v) PE, and 1 μM C100Flag substrate adjusted to 0.5% SDS prior to addition to the reactions. Aβ40 and Aβ42 generated in each reaction were measured by ELISA as described in the Experimental Procedures ($n = 3$).

concentrations (0.0125−0.2%) of each of these lipids did not alter the Aβ42/Aβ40 ratios, which were 0.12−0.14 for this experiment (data not shown). These ratios are similar to the values reported for Aβ peptides secreted from cultured neuronal cells (*48*), generated in vitro with solubilized membranes (*32*), or obtained from wild-type human cells and fluids (*27*). Taken together, these observations suggest that total γ-secretase activity (Aβ40 + Aβ42), but not cleavage site specificity (Aβ42/Aβ40 ratio), can be modulated by individually varying the concentrations of PC and SM. Next, to determine whether the increases of γ-secretase activity observed with PC and SM were additive, we evaluated the effect of various concentrations of SM in the presence of 0.1% PC + 0.025% PE. When compared to samples that did not contain SM, a further 1.25-fold increase ($P < 0.01$) in Aβ40 production and a 1.55-fold increase

($P < 0.0001$) in Aβ42 production were observed when 0.05% SM was added (Figure 4B). These data could suggest that SM, in the presence of 0.1% PC + 0.025% PE, preferentially elevates Aβ42 production when compared to that of Aβ40. As several reports exist on the cholesterol dependence of γ-secretase (*49*−*53*), we decided to include an examination of cholesterol in our analysis of the influence of lipids on the purified γ-secretase. A technical limitation in addressing this question is the poor solubility of cholesterol in the detergents (CHAPSO or Digitonin) or solvents (DMSO or ethanol) known to be compatible with γ-secretase activity. We therefore decided to test a mixture of 10 volumes of chloroform, 10 volumes of methanol, and 3 volumes of water (10:10:3), which is known to solubilize all membrane lipids, including cholesterol and glycosylphosphatidylinositol (*54*), for compatibility with γ-secretase activity. We found that when included in our in vitro activity assay, 10:10:3 (final concentration of both chloroform and methanol is 0.6%) affected γ-secretase activity (Figure 4C). The presence of 10:10:3 resulted in a 65% decrease of Aβ40 production and a 33% decrease of Aβ42 production (Figure 4C), suggesting that Aβ40 formation was more sensitive to chloroform and/or methanol than Aβ42 formation was. Despite this decrease of activity observed in the presence of 0.6% chloroform and methanol, residual γ activity was readily detectable in our in vitro activity assay (Figure 4C). We therefore assessed the effects of various concentrations of cholesterol on the purified γ-secretase activity. We found that increasing concentrations of cholesterol (from 0 to 0.025%) improved production of both Aβ40 and Aβ42 (a ∼2-fold increase in both Aβ40 and Aβ42 when compared to the 10:10:3 control), whereas higher concentrations (0.05% and above) promoted a decrease of those activities (Figure 4C). Under our in vitro activity assay conditions, cholesterol concentrations equal or higher to 0.05% promoted protein aggregation (data not shown), which may well explain the loss of γ-secretase activity. These data suggest that cholesterol, like PC and SM, can improve γ-secretase activity without changing its cleavage specificity. However, because of the negative effect of the 10:10:3 solvent on γ-secretase activity, we cannot exclude that the increased activity observed in the presence of low concentrations of cholesterol was due to a rescue of activity lost because of the solvents.

On the basis of all of the results described previously and the standard conditions reported in CHAPSO-solubilized HeLa cell membranes (*30*), we used 0.1% PC and 0.025% PE for all subsequent γ-secretase reactions.

Detergent Dependence of Aβ40 and Aβ42 Formation by Purified γ-Secretase. To assess whether various concentrations of different detergents affect the purified γ-secretase efficiency, in vitro reactions were run with the purified enzyme solubilized at 10-fold dilution from stock in HEPES buffers (pH 7.5) containing 0.10−1% CHAPSO or 0.01−1% digitonin. As shown in Figure 4D, our experiments revealed optimal cleavage activity at Aβ40 (9.8 pM/min) when γ-secretase was solubilized in 0.1 or 0.25% CHAPSO, whereas concentrations of 0.5% CHAPSO or higher were associated with much less or no activity. As shown in Figure 4E, optimal cleavage activity at Aβ40 (3.4 and 2.8 pM/min, respectively) was achieved in 0.01 or 0.05% digitonin, whereas a concentration higher than 0.2% was incompatible with activity (Figure 4E). Interestingly, the Aβ42/Aβ40 cleavage ratios obtained in 0.1% CHAPSO and 0.01% digitonin (0.16 and 0.11, respectively) were closely similar to the physiological ratios mentioned previously. However, we found that the solubilization of the purified enzyme in 0.25% CHAPSO resulted in a selective 2-fold increase in Aβ42 when compared to 0.1% CHAPSO (2.8 pM/min in 0.25% CHAPSO and 1.6 pM/min in 0.1% CHAPSO) (Figure 4D). Because the activity for Aβ40 is the same in both 0.1 and 0.25% CHAPSO, but the activity for Aβ42 is 2-fold higher in 0.25 than 0.1% CHAPSO, the corresponding Aβ42/Aβ40 cleavage ratios are different (0.16 in 0.1% and 0.30 in 0.25% CHAPSO). When compared to the optimal Aβ40 activity found in 0.01% digitonin (3.4 pM/min), a 2.8-fold increased activity is found in 0.1% CHAPSO (9.8 pM/min) (compare different scales on the ordinates of Figure 4D,E), suggesting that CHAPSO favors a more active enzymatic conformation than does digitonin.

Kinetics of Purified γ-Secretase: K_m and V_{max}. Because purification of γ-secretase close to homogeneity has not previously been reported, we decided to study the detailed enzyme kinetics of our preparation. As shown in Figure 5A, the time dependence of Aβ40 formation by purified γ-secretase was linear for at least 3.5 h under our experimental conditions, suggesting that the purified enzyme was stable and that the substrate was in excess during the experiments. The apparent K_m and V_{max} for the processing of C100Flag substrate to Aβ40 by purified γ-secretase diluted 1:10 (v/v) in 0.1% CHAPSO-HEPES, pH 7.5, is 0.70 μM and 11.8 pM/min, respectively (Figure 5B). The apparent K_m for the processing of C100Flag substrate to Aβ40 by purified γ-secretase diluted 1:10 (v/v) in 0.05% digitonin-HEPES, pH 7.5, is 1.00 μM (data not shown). These K_m values are in the range of K_m values reported previously with non-purified γ-secretase microsomal preparations using C100 substrate (0.23 μM) (*55*) or Flag-tagged C100 substrate (1 μM) (*32*).

pH Dependence of Aβ40 and Aβ42 Formation by Purified γ-Secretase. Studying the pH dependence of purified γ-secretase diluted 1:5 (v/v) in 0.25% CHAPSO (Figure 5C) or 0.05% digitonin (data not shown) yielded a pH optimum of 7.5. We found closely similar activity at pH 7.0 and 7.5 (23 and 28 pM/min, respectively), consistent with the report of an optimum pH value of 7.0 (*32*). Interestingly, the more the pH changes from the optimum value of 7.5, the more the Aβ42/Aβ40 ratio increased (0.33 at pH 7.5 as compared to 0.46 at pH 6.0 or 0.38 at pH 9.0, Figure 5C), suggesting that the Aβ40 cleavage activity is more pH sensitive than Aβ42 activity. We observed similar results using γ-secretase solubilized in 0.05% digitonin, which showed an Aβ42/Aβ40 ratio of 0.15 at pH 7.5, 0.21 at pH 6.0, and 0.38 at pH 8.5 (data not shown).

Purified γ-Secretase and Notch Cleavage. We recently reported that C100Flag and N100Flag, which are analogous APP- and Notch-based substrates, inhibited the cleavage of each other, indicating that the same γ-secretase complex can cleave either protein (*30*). To confirm this observation, we probed the purified enzyme for N100Flag cleavage and found that purified γ-secretase cleaves N100Flag into appropriate products, analogous to those seen from CHAPSO-solubilized HeLa cell membranes (data not shown).

Inhibition of Purified γ-Secretase Activity by DAPT, III-31C, and Sulindac Sulfide. Next, we examined the effects

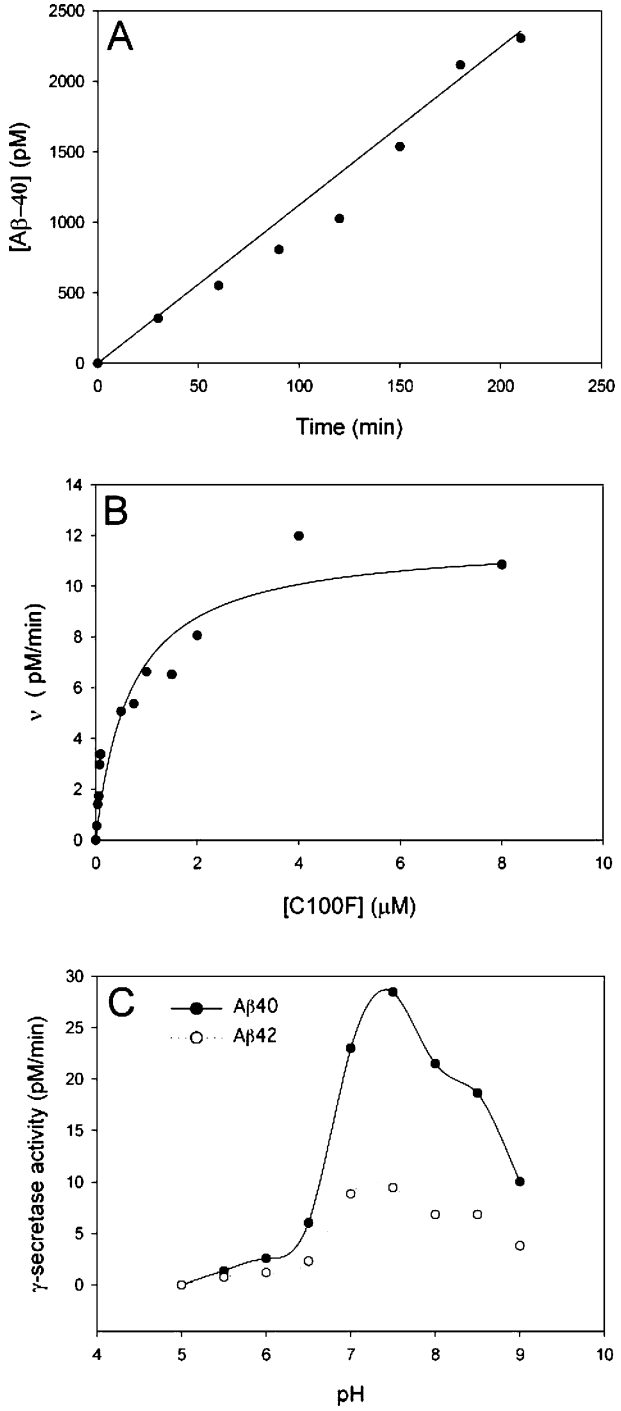

FIGURE 5: Kinetics of purified γ-secretase activity on C100Flag. (A) Typical time dependence of Aβ40 formation at 37 °C by purified γ-secretase diluted in 0.1% CHAPSO-HEPES, pH 7.5, and in the presence of 1 μM C100Flag substrate adjusted to 0.5% SDS prior to addition to the reactions. (B) Typical Aβ40 formation as a function of C100Flag concentration after 180 min incubation at 37 °C. (C) Typical Aβ40 and Aβ42 formation as a function of pH by purified γ-secretase diluted in 0.25% CHAPSO-HEPES after 180 min incubation at 37 °C and in the presence of 1 μM C100Flag substrate adjusted to 0.5% SDS prior to addition to the reactions. For all the kinetic experiments, 0.1% PC and 0.025% PE were added to the reactions, and Aβ40 and Aβ42 were measured by ELISA as described in the Experimental Procedures.

of two well-characterized γ-secretase inhibitors, III-31C (*31*) and DAPT (*56*) on the cleavage efficiency of the purified enzyme on C100Flag. III-31C inhibited the generation of both Aβ40 and Aβ42 in a concentration-dependent fashion

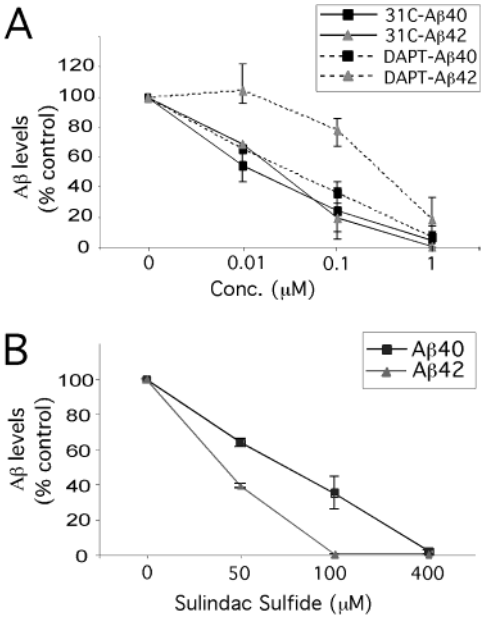

FIGURE 6: Effect of characterized inhibitors on Aβ40 and Aβ42 generation by purified γ-secretase. γ-Secretase diluted in 0.1% CHAPSO-HEPES, pH 7.5, was incubated at 37 °C for 180 min in the presence of 1 μM C100Flag substrate (adjusted to 0.5% SDS prior to addition to the reactions); 0.1% PC; 0.025% PE; and 0.01, 0.1, or 1 μM III-31C or DAPT ($n = 3$) (A); or 50, 100, or 400 μM sulindac sulfide ($n = 3$) (B). Aβ40 and Aβ42 were measured by ELISA.

and with a similar potency, with IC_{50} values of 20 nM for Aβ40 and 40 nM for Aβ42 (Figure 6A). Interestingly, DAPT was more effective against Aβ40 (IC_{50} value of 60 nM) than Aβ42 (IC_{50} value of 400 nM) (Figure 6A). At 10 nM DAPT, Aβ40 formation was considerably blocked, while the level of Aβ42 was similar (or even higher) from that of the control (Figure 6A). Similar effects have been reported for other γ-secretase inhibitors including Calpain (*57*) and difluoro ketone peptidomimetic 1 (*58*). We also examined the effect of sulindac sulfide, a nonsteroidal antiinflammatory drug (NSAID) reported to preferentially decrease production of the highly amyloidogenic Aβ42 peptide (*59*). We found that sulindac sulfide inhibited both Aβ40 and Aβ42 generation, with IC_{50} values of 70 and 40 μM, respectively (Figure 6B). These IC_{50} values are consistent with recently reported IC_{50} values of sulindac sulfide for inhibiting both Aβ42 generation ($IC_{50} = 20.2$ μM) and Aβ40 generation (IC_{50} between 50 and 100 μM) in vitro (*60*). Our data on purified γ-secretase strongly suggest that the γ-secretase complex is a direct target of sulindac sulfide.

SDS Treatment of the C100Flag Substrate Influences the Cleavage Specificity of Purified γ-Secretase. To determine the precise γ-cleavage sites, Aβ-peptides were first generated by purified γ-secretase as described in the Experimental Procedures, except that the C100Flag substrate was not adjusted to 0.5% SDS prior to addition to the reaction (to avoid potential SDS interference with the mass spectral analysis of the resultant peptides), and the purified enzyme was not diluted (from the stock solution recovered after the anti-M2 affinity step, Figure 3A, step 5). The Aβ-cleavage products were immunoprecipitated with monoclonal anti-Aβ antibody 4G8 and subsequently analyzed by MALDI-TOF mass spectrometry. The MS spectrum revealed principally Aβ 1-40, 1-42, and 1-43 but also shorter species

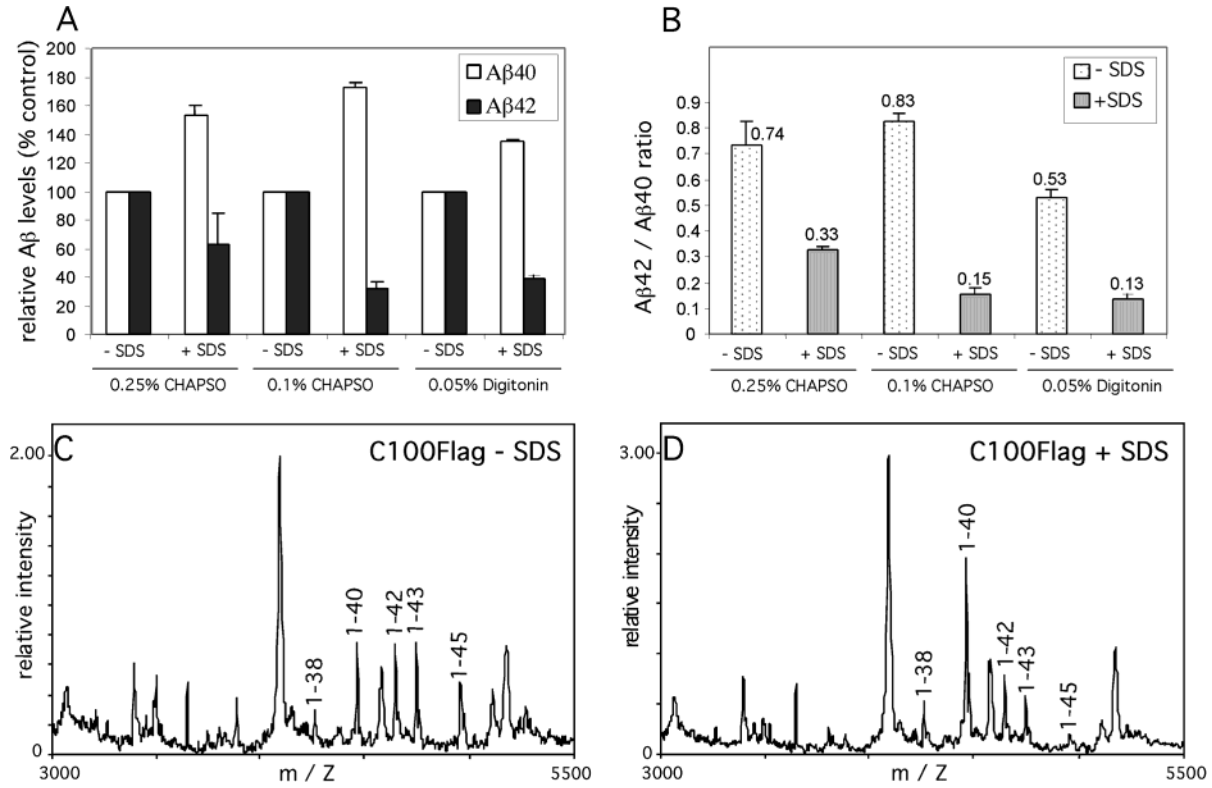

FIGURE 7: SDS treatment of the C100Flag substrate influences the cleavage specificity by purified γ-secretase. (A) γ-Secretase diluted in three different buffers (0.25% CHAPSO-HEPES, pH 7.5, 0.1% CHAPSO-HEPES, pH 7.5, or 0.05% digitonin-HEPES, pH 7.5) was incubated at 37 °C for 180 min in the presence of 0.1% PC, 0.025% PE, and 1 μM C100Flag substrate adjusted (+SDS) or not (−SDS) to 0.5% SDS prior to addition to the reactions (final SDS concentration in the C100Flag assay is 0.0085%). Aβ40 and Aβ42 were measured by ELISA and were normalized to the values obtained in absence of SDS (control = 100%) (n = 4). (B) The ratios of Aβ42/Aβ40 were calculated for each condition described above. (C and D) Mass spectral analysis of Aβ peptides generated from C100Flag adjusted (D) or not (C) to 0.5% SDS prior the addition to the reaction. The γ-secretase cleavage products were captured with monoclonal anti-Aβ antibody 4G8 and subjected to MALDI-TOF analysis using a Voyager-DE STR mass spectrometer. All Aβ-related peptides are labeled.

(Aβ 1-38) and longer species (Aβ 1-45), and surprisingly, the Aβ 1-42/Aβ1-40 cleavage ratio (as estimated by ELISA) was much higher than expected (0.80, data not shown). This high Aβ1-42/Aβ1-40 cleavage ratio also observed on the mass spectrum was unexpected and in apparent contrast with the Aβ1-42/Aβ1-40 ratios quantified by ELISA (between 0.10 and 0.26) and observed in the experiments reported previously (Figures 4−6). However, samples submitted for ELISA quantification were always prepared with C100Flag substrates that had been adjusted to 0.5% SDS (final SDS concentration in the C100Flag assay was 0.0085%), heated at 65 °C for 5 min, and then spun at 14 000 rpm for 1 min to pellet insoluble substrate aggregates prior to the assay. In contrast, no SDS has been added to the C100Flag substrates used for the samples prepared for the MS analysis of the Aβ species. Because the presence or absence of SDS as well as the heating step were the only differences between these two reactions, we first examined the effect of this ionic detergent on γ-secretase cleavage specificity. To do so, we ran in vitro reactions with purified γ-secretase solubilized by diluting 10-fold from stock in defined buffers containing 0.25% CHAPSO or 0.1% CHAPSO or 0.05% digitonin and with the C100Flag substrate pretreated or not with 0.5% SDS. After 4 h incubation at 37 °C, Aβ40 and Aβ42 were quantified by ELISA. We found that in all three detergent buffers, pretreatment of the C100Flag substrates with 0.5% SDS specifically increased the amount of Aβ40 cleavage (153, 173, and 135%, respectively, when normalized to the Aβ40 amount in the reactions without SDS) and decreased the amount of Aβ42 cleavage (63, 31, and 38%, respectively, when normalized to the Aβ42 amount in the reactions without SDS) (Figure 7A). However, the total cleavage activity (Aβ40 + Aβ42) was conserved in each condition, suggesting that SDS does not promote a gain or loss of function of the enzyme but rather a shift of cleavage specificity. We also quantified the Aβ1-42/ Aβ1-40 cleavage ratios in all reactions. Reactions run with purified γ-secretase in defined buffers containing 0.25% CHAPSO, 0.1% CHAPSO, or 0.05% digitonin and with C100Flag substrates preincubated in 0.5% SDS showed Aβ1-42/Aβ1-40 cleavage ratios of 0.33, 0.15, and 0.13, respectively (Figure 7B). These Aβ1-42/ Aβ1-40 values are in good agreement with the ratios estimated in the experiments described in Figure 4D,E (0.30, 0.16, and 0.04). In contrast, reactions run in the same conditions as described previously, except that the C100Flag substrates were not adjusted to 0.5% SDS prior to addition to the reactions, show Aβ1-42/Aβ1-40 cleavage ratios of 0.74, 0.83, and 0.53, respectively (Figure 7B). Interestingly, the effect of SDS on Aβ1-40 and Aβ1-42 production is more pronounced when the enzyme was diluted in 0.1% CHAPSO than in 0.25% CHAPSO (compare the two conditions in Figure 7B), supporting the different Aβ1-42/Aβ1-40 cleavage ratios found in these conditions in Figure 4D (0.16 when the enzyme is diluted in 0.1% CHAPSO and 0.30 when diluted in 0.25% CHAPSO). Finally, we confirmed the effect of SDS on the specific γ-secretase cleavage by using mass spectrometry to analyze side-by-side the Aβ-species generated in vitro in two different reactions: one performed with

and the other without preincubating C100Flag in 0.5% SDS. As shown in Figure 7C, in absence of SDS, Aβ40, Aβ42, and Aβ43 strikingly resulted in the same peak heights. The addition of SDS to the substrate promotes an increase in the Aβ40 cleavage and a decrease in Aβ42, Aβ43, and Aβ45 cleavages (Figure 7D), confirming the shift of cleavage specificity observed by ELISA (Figure 7A,B). Next, we found that reactions run with C100Flag substrate heated or not at 65 °C for 5 min (in both conditions not adjusted to 0.5% SDS) showed similar Aβ1-42/Aβ1-40 ratios (data not shown), excluding any effect of the heating step on the cleavage specificity.

Taken together, these data clearly suggest an important role of conformational alterations (in this case induced by SDS) on the specificity of the γ-cleavage, leading in vitro to a shift from a disease-promoting pattern (Aβ1-42/Aβ1-40 ratios between 0.80 and 1.0) to a more physiological pattern (Aβ1-42/Aβ1-40 ratios between 0.10 and 0.20).

DISCUSSION

We report here a detailed procedure for the high-grade purification of active human γ-secretase. Extensive mass spectral analysis of the purified proteins separated under denaturing conditions revealed PS1-NTF, PS1-CTF, Aph1, NCT, and Pen-2 as the predominant proteins identified in the fraction recovered in the final purification step. ATP/ADP translocase (ANT, NCBI accession number 399012), choline transporter (CD92, 16945323), prohibitin (1673514), PS1-isoform 374 (7549815), transferrin receptor (4507457), and IgG (21304449) were also identified in the same fraction, although in apparently smaller amounts. Our identification by LC-MS-MS of a peptide that is specific to PS1-374, a shorter isoform of PS1 (-TLLQRMMMAGSVR-, corresponding to residues 353−365 of PS1-374) suggests that this protein was specifically present in the purified fraction. To our knowledge, PS1-374 has never before been associated with active γ-secretase. Transferrin receptor (TfR, for a review, see ref *61*) is overexpressed in the PS70 stable CHO cell line (*62*), the parental cell line we used to generate the γ-30 and S-1 cell lines (*12*, *29*). We found that TfR could coimmunoprecipitate with PS1-holoprotein but only in stable cell lines overexpressing both proteins, suggesting a nonspecific protein−protein interaction (data not shown). IgG (immunoglobulin γ 1 heavy chain) was the major contaminating protein found in our preparations (Figure 1C and Supporting Information Figure 2) resulting from some M2-anti-Flag antibodies that were coupled to the M2-anti-Flag affinity resin and then nonspecifically eluted by the Flag peptides during the purification procedure. Importantly, we were not able to coprecipitate ANT, CD92, prohibitin, PS1-374, or TfR with PS1-NTF in a 1% CHAPSO-solubilized CHO lysate, and none of the other endogenous γ-secretase components coprecipitated with those proteins either, strongly suggesting that they do not interact specifically with γ-secretase. Nevertheless, we cannot exclude the small possibility that one or more of the identified proteins may interact in some way with γ-secretase. Further genetic and biochemical analyses performed with additional antibodies raised against different domains of these proteins will be necessary to address this question. At present, we consider these other membrane proteins, which were never visualized by silver staining, as likely trace contaminants in our purified preparations. Taken together, our data strongly suggest that PS1-NTF, PS1-CTF, Aph1, NCT, and Pen-2 are sufficient for the formation of the active γ-secretase complex.

We also identify here certain conditions that are critical for the specificity of γ-secretase cleavage of APP by purified γ-secretase. Understanding the determinants of cleavage specificity remains a priority because modulation of such determinants could prevent or treat AD, which is strongly associated with excessive Aβ42 accumulation in the brain. Moreover, the detailed molecular mechanism by which FAD-causing missense mutations in presenilin increase Aβ-42 production remains unclear. Murphy et al. (*63*) favor a model of γ-secretase function in which the overproduction of longer forms of Aβ by PS1 FAD mutants is dependent on the membrane positioning of the substrate relative to the active site. Consistent with this idea, Lichtenthaler et al. (*64*) identified the length of the whole TMD of C99 as a major determinant of the specific γ-cleavage site. Interestingly, they found that for C99-ΔNT (two residues deleted at the N-terminal end of the TMD of C99), the γ-cleavage site was shifted in the C-terminal direction, increasing the processing of the deleted substrate to Aβ1-42 and Aβ1-43. Consistent with this observation, we show here that, when C100Flag substrate is incubated with γ-secretase in the absence of SDS, the enzyme generates unusually high amounts of Aβ1-42 and Aβ1-43. This observation indicates that SDS, a detergent that mimics some characteristics of biological membranes and is commonly used to model membrane and other hydrophobic environments, alters γ-secretase cleavage specificity. SDS has been shown to induce particular secondary structures, particularly α-helices, in polypeptides (*65*, *66*). SDS has also been shown to improve the assembly and stability of integral membrane protein complexes such as OmpF porin (*67*) and the folding and stability of membrane proteins such as bacteriorhodopsin and DsbB (*68*, *69*).

It has been shown that overexpression of wild-type *Drosophila melanogaster* PS is associated with a drastic overproduction of Aβ 1-42 from human APP in murine N2a cells but not in *Drosophila* S2 cells (*70*). The authors suggest that differences in the composition and metabolism of membrane lipids between mammalian and *Drosophila* cells could underlie the distinct behaviors observed in Aβ1-42 generation. In this regard, we found that the lipids, PC and SM, were able to markedly improve the efficiency of purified γ-secretase on the APP-based substrate, whereas PE had very little or no effect. We also found that SM, in the presence of 0.1% PC + 0.025% PE, preferentially potentiated Aβ42 production when compared to Aβ40 production and that cholesterol appeared to improve purified γ-secretase activity. Specifically, our data show that (1) 0.1% PC + 0.025% PE did not correct the overproduction of Aβ42 and Aβ43 by purified γ-secretase from C100Flag lacking SDS and (2) 0.1% PC + 0.025% PE drastically increased production of total Aβ (Aβ40 + Aβ42) from SDS-treated C100Flag without affecting the (physiological) Aβ-42/Aβ-40 ratio of 0.10−0.15. An attractive hypothesis emerging from these data is that the lipids PC and SM help regulate the active site conformation of γ-secretase but not the structure of the C100Flag substrate, whereas the latter is affected by the presence of SDS. These observations are consistent with a model in which the cleavage specificity depends on the conformation and position in the plasma membrane of the

C99 substrate, which is controlled in our in vitro assay by SDS, a detergent that mimics some characteristics of biological membranes, whereas the total amount of γ-secretase cleavage depends on the concentration of lipids such as PC or SM. It would be interesting to identify one or more endogenous SDS-mimicking factor(s) in cells that can similarly control the conformation of the APP TMD and other substrates.

In conclusion, the availability of a specific, well-defined, and reproducible protocol for the high-grade purification of the γ-secretase complex should enable further rapid progress in deciphering the detailed enzyme kinetics on numerous physiological substrates and the factors that regulate the cleavage specificity of this fascinating intramembrane protease, with attendant therapeutic insights for the design of safe and effective inhibitors.

ACKNOWLEDGMENT

We thank S. Gandy for PS1 antibody Ab14; D. Miller and P. Savam for the NCT antibody, R302; and H. Mori for the PS1-isoform 374 antibodies. We are also grateful to J. Strahle, B. Zheng, and W. Xia for ELISA analysis.

SUPPORTING INFORMATION AVAILABLE

Tables of data for human NCT, PEN-2, Aph1α2, and PS1, mass spectral identification of γ-secretase-associated proteins, and purification of γ-secretase from S-1 cells and mass spectral identification of its associated proteins. This material is available free of charge via the Internet at http://pubs.acs.org.

REFERENCES

1. Selkoe, D. (2001) Alzheimer's Disease: Genes, Proteins, and Therapy, *Physiol. Rev. 81*, 741−66.
2. Vassar, R., and Citron, M. (2000) Abeta-generating enzymes: recent advances in β- and γ-secretase research, *Neuron 27*, 419−22.
3. Wolfe, M. S., De Los Angeles, J., Miller, D. D., Xia, W., and Selkoe, D. J. (1999) Are presenilins intramembrane-cleaving proteases? Implications for the molecular mechanism of Alzheimer's disease, *Biochemistry 38*, 11223−30.
4. Wolfe, M. S., and Selkoe, D. (2002) Biochemistry. Intramembrane proteases—mixing oil and water, *Science 296*, 2156−7.
5. De Strooper, B., Saftig, P., Craessaerts, K., Vanderstichele, H., Gundula, G., Annaert, W., Von Figura, K., and Van Leuven, F. (1998) Deficiency of presenilin-1 inhibits the normal cleavage of amyloid precursor protein, *Nature 391*, 387−90.
6. Wolfe, M. S., Xia, W., Ostaszewski, B. L., Diehl, T. S., Kimberly, W. T., and Selkoe, D. J. (1999) Two transmembrane aspartates in presenilin-1 required for presenilin endoproteolysis and γ-secretase activity, *Nature 398*, 513−7.
7. De Strooper, B., Annaert, W., Cupers, P., Saftig, P., Craessaerts, K., Mumm, J. S., Schroeter, E. H., Schrijvers, V., Wolfe, M. S., Ray, W. J., Goate, A., and Kopan, R. (1999) A presenilin-1-dependent γ-secretase-like protease mediates release of Notch intracellular domain, *Nature 398*, 518−22.
8. Struhl, G., and Greenwald, I. (1999) Presenilin is required for activity and nuclear access of Notch in *Drosophila*, *Nature 398*, 522−5.
9. Ye, Y., Lukinova, N., and Fortini, M. E. (1999) Neurogenic phenotypes and altered Notch processing in *Drosophila* presenilin mutants, *Nature 398*, 525−9.
10. Francis, R., McGrath, G., Zhang, J., Ruddy, D. A., Sym, M., Apfeld, J., Nicoll, M., Maxwell, M., Hai, B., Ellis, M. C., Parks, A. L., Xu, W., Li, J., Gurney, M., Myers, R. L., Himes, C. S., Hiebsch, R., Ruble, C., Nye, J. S., and Curtis, D. (2002) aph-1 and pen-2 are required for Notch pathway signaling, γ-secretase cleavage of βAPP, and presenilin protein accumulation, *Dev. Cell 3*, 85−97.
11. Takasugi, N., Tomita, T., Hayashi, I., Tsuruoka, M., Niimura, M., Takahashi, Y., Thinakaran, G., and Iwatsubo, T. (2003) The role of presenilin cofactors in the γ-secretase complex, *Nature 422*, 438−41.
12. Kimberly, W. T., LaVoie, M., Ostaszewski, B. L., Ye, W., Wolfe, M. S., and Selkoe, D. J. (2003) γ-Secretase is a membrane protein complex comprised of presenilin, nicastrin, Aph-1, and Pen-2, *Proc. Natl. Acad. Sci. U.S.A. 100*, 6382−7.
13. Edbauer, D., Winkler, E., Regula, J. T., Pesold, B., Steiner, H., and Haass, C. (2003) Reconstitution of γ-secretase activity, *Nat. Cell Biol. 5*, 486−8.
14. Wolfe, M. (2002) Therapeutic strategies for Alzheimer's disease, *Nat. Rev. Drug Discov. 1*, 859−66.
15. Edbauer, D., Winkler, E., Haass, C., and Steiner, H. (2002) Presenilin and nicastrin regulate each other and determine amyloid β-peptide production via complex formation, *Proc. Natl. Acad. Sci. U.S.A. 99*, 8666−71.
16. Farmery, M. R., Tjernberg, L., Pursglove, S. E., Bergman, A., Winblad, B., and Naslund, J. (2003) Partial purification and characterization of γ-secretase from post-mortem human brain, *J. Biol. Chem. 278*, 24277−84.
17. Nyabi, O., Bentahir, M., Horre, K., Herreman, A., Gottardi-Littell, N., Van Broeckhoven, C., Merchiers, P., Spittaels, K., Annaert, W., and De Strooper, B. (2003) Presenilins mutated at Asp-257 or Asp-385 restore Pen-2 expression and Nicastrin glycosylation but remain catalytically inactive in the absence of wild-type presenilin, *J. Biol. Chem. 278*, 43430−6.
18. Ni, C. Y., Murphy, M., Golde, T. E., and Carpenter, G. (2001) γ-Secretase cleavage and nuclear localization of ErbB-4 receptor tyrosine kinase, *Science 294*, 2179−81.
19. Marambaud, P., Shioi, J., Serban, G., Georgakopoulos, A., Sarner, S., Nagy, V., Baki, L., Wen, P., Efthimiopoulos, S., Shao, Z., Wisniewski, T., and Robakis, N. K. (2001) A presenilin-1/γ-secretase cleavage releases the E-cadherin intracellular domain and regulates disassembly of adherens junctions, *EMBO J. 21*, 1948−56.
20. Kim, D. Y., Ingano, L., and Kovacs, D. M. (2002) Nectin-1alpha, an immunoglobulin-like receptor involved in the formation of synapses, is a substrate for presenilin/γ-secretase-like cleavage, *J. Biol. Chem. 277*, 49976−81.
21. May, P., Reddy, Y., and Herz, J. (2002) Proteolytic processing of low-density lipoprotein receptor-related protein mediates regulated release of its intracellular domain, *J. Biol. Chem. 277*, 18736−43.
22. Lammich, S., Okochi, M., Takeda, M., Kaether, C., Capell, A., Zimmer, A. K., Edbauer, D., Walter, J., Steiner, H., and Haass, C. (2002) Presenilin-dependent intramembrane proteolysis of CD44 leads to the liberation of its intracellular domain and the secretion of an Abeta-like peptide, *J. Biol. Chem. 277*, 44754−9.
23. LaVoie, M. J., and Selkoe, D. (2003) The Notch ligands, Jagged and Delta, are sequentially processed by α-secretase and presenilin/γ-secretase and release signaling fragments, *J. Biol. Chem. 278*, 34427−37.
24. Suzuki, N., Cheung, T., Cai, X. D., Odaka, A., Otvos, L., Jr., Eckman, C., Golde, T. E., and Younkin, S. G. (1994) An increased percentage of long amyloid β-protein secreted by familial amyloid β-protein precursor (β APP717) mutants, *Science 264*, 1336−40.
25. Borchelt, D. R., Thinakaran, G., Eckman, C. B., Lee, M. K., Davenport, F., Ratovitsky, T., Prada, C. M., Kim, G., Seekins, S., Yager, D., Slunt, H. H., Wang, R., Seeger, M., Levey, A. I., Gandy, S. E., Copeland, N. G., Jenkins, N. A., Price, D. L., Younkin, S. G., and Sisodia, S. (1996) Familial Alzheimer's disease-linked presenilin 1 variants elevate Abeta1-42/1-40 ratio in vitro and in vivo, *Neuron 17*, 1005−13.
26. Duff, K., Eckman, C., Zehr, C., Yu, X., Prada, C. M., Perez-tur, J., Hutton, M., Buee, L., Harigaya, Y., Yager, D., Morgan, D., Gordon, M., Holcomb, L., Refolo, L., Zenk, B., Hardy, J., and Younkin S. (1996) Increased amyloid-β42(43) in brains of mice expressing mutant presenilin 1, *Nature 383*, 710−3.
27. Scheuner, D., Eckman, C., Jensen, M., Song, X., Citron, M., Suzuki, N., Bird, T. D., Hardy, J., Hutton, M., Kukull, W., Larson, E., Levy-Lahad, E., Viitanen, M., Peskind, E., Poorkaj, P., Schellenberg, G., Tanzi, R., Wasco, W., Lannfelt, L., Selkoe, D., and Youkin, S. (1996) Secreted amyloid β-protein similar to that in the senile plaques of Alzheimer's disease is increased in vivo by thepresenilin 1 and 2 and APP mutations linked to familial Alzheimer's disease, *Nat. Med. 2*, 864−70.
28. Citron, M., Westaway, D., Xia, W., Carlson, G., Diehl, T., Levesque, G., Johnson-Wood, K., Lee, M., Seubert, P., Davis,

A., Kholodenka, D., Motter, R., Sherrington, R., Perry, B., Yao, H., Strome, R., Lieberburg, I., Rommens, J., Kim, S., Schenk, D., Fraser, P., St. George-Hyslop, P., and Selkoe, D. J. (1997) Mutant presenilins of Alzheimer's disease increase production of 42-residue amyloid β-protein in both transfected cells and transgenic mice, *Nat. Med. 3*, 67−72.

29. Fraering, P. C., LaVoie, M., Ye, W., Ostaszewski, B. L., Kimberly, W. T., Selkoe, D. J., and Wolfe, M. S. (2004) Detergent-dependent dissociation of active γ-secretase reveals an interaction between Pen-2 and PS1-NTF and offers a model for subunit organization within the complex, *Biochemistry 43*, 323−33.
30. Kimberly, W. T., Esler, W., Ye, W., Ostaszewski, B. L., Gao, J., Diehl, T., Selkoe, D. J., and Wolfe, M. S. (2003) Notch and the amyloid precursor protein are cleaved by similar β-secretase(s), *Biochemistry 42*, 137−44.
31. Esler, W. P., Kimberly, W., Ostaszewski, B. L., Ye, W., Diehl, T. S., Selkoe, D. J., and Wolfe, M. S. (2002) Activity-dependent isolation of the presenilin−γ-secretase complex reveals nicastrin and a γ substrate, *Proc. Natl. Acad. Sci. U.S.A. 99*, 2720−5.
32. Li, Y. M., Lai, M., Xu, M., Huang, Q., DiMuzio-Mower, J., Sardana, M. K., Shi, X. P., Yin, K. C., Shafer, J. A., and Gardell, S. J. (2000) Presenilin 1 is linked with γ-secretase activity in the detergent solubilized state, *Proc. Natl. Acad. Sci. U.S.A. 97*, 6138−43.
33. Xia, W., Zhang, J., Ostaszewski, B. L., Kimberly, W. T., Seubert, P., Koo, E. H., Shen, J., and Selkoe, D. J. (1998) Presenilin 1 regulates the processing of β-amyloid precursor protein C-terminal fragments and the generation of amyloid β-protein in endoplasmic reticulum and Golgi, *Biochemistry 37*, 16465−71.
34. Wang, R., Sweeney, D., Gandy, S. E., and Sisodia, S. S. (1996) The profile of soluble amyloid β-protein in cultured cell media. Detection and quantificaiton of amyloid β-protein and variants by immunoprecipitation−mass spectrometry, *J. Biol. Chem. 271*, 31894−31902.
35. LaVoie, M. J., Fraering, P. C., Ostaszewski , B. L., Ye, W., Kimberly, W. T., Wolfe, M. S., and Selkoe, D. J. (2003) Assembly of the γ-secretase complex involves early formation of an intermediate subcomplex of Aph-1 and nicastrin, *J. Biol. Chem. 278*, 37213−22.
36. Fujiki, Y., Hubbard, A. L., Fowler, S., and Lazarow, P. B. (1982) Isolation of intracellular membranes by means of sodium carbonate treatment: Application to endoplasmic reticulum, *J. Cell Biol. 93*, 97−102.
37. Capell, A., Grunberg, J., Pesold, B., Diehlmann, A., Citron, M., Nixon, R., Beyreuther, K., Selkoe, D. J., and Haass, C. (1998) The proteolytic fragments of the Alzheimer's disease-associated presenilin-1 form heterodimers and occur as a 100−150 kDa molecular mass complex, *J. Biol. Chem. 273*, 3205−11.
38. Yu, G., Chen, F., Levesque, G., Nishimura, M., Zhang, D. M., Levesque, L., Rogaeva, E., Xu, D., Liang, Y., Duthie, M., St. George-Hyslop, P. H., and Fraser, P. E. (1998) The presenilin 1 protein is a component of a high molecular weight intracellular complex that contains β-catenin, *J. Biol. Chem. 273*, 16470−5.
39. Sahara, N., Yahagi, Y., Takagi, H., Kondo, T., Okochi, M., Usami, M., Shirasawa, T., and Mori, H. (1996) Identification and characterization of presenilin I-467, I-463, and I-374, *FEBS Lett. 381*, 7−11.
40. Kimberly, W. T., LaVoie, M., Ostaszewski, B. L., Ye, W., Wolfe, M. S., and Selkoe, D. J. (2002) Complex N-linked glycosylated nicastrin associates with active γ-secretase and undergoes tight cellular regulation, *J. Biol. Chem. 277*, 35113−7.
41. Yang, D. S., Tandon, A., Chen, F., Yu, G., Yu, H., Arawaka, S., Hasegawa, H., Duthie, M., Schmidt, S. D., Ramabhadran, T. V., Nixon, R. A., Mathews, P. M., Gandy, S. E., Mount, H. T., St. George-Hyslop, P. H., and Fraser, P. E. (2002) Mature glycosylation and trafficking of nicastrin modulate its binding to presenilins, *J. Biol. Chem. 277*, 28135−42.
42. Leem, J. Y., Vijayan, S., Han, P., Cai, D., Machura, M., Lopes, K. O., Veselits, M. L., Xu, H., and Thinakaran, G. (2002) Presenilin 1 is required for maturation and cell surface accumulation of nicastrin, *J. Biol. Chem. 277*, 19236−40.
43. Kim, T. W., Pettingel, W., Jung, Y. K., Kovacs, D. M., and Tanzi, R. E. (1997) Alternative cleavage of Alzheimer-associated presenilins during apoptosis by a caspase-3 family protease, *Science 277*, 373−6.
44. Hartmann, H., Busciglio, J., Baumann, K.-H., Staufenbiel, M., and Yankner, B. A. (1997) Developmental Regulation of Presenilin-1 Processing in the Brain Suggests a Role in Neuronal Differentiation, *J. Biol. Chem. 272*, 14505−8.
45. Nitsch, R. M., Blusztajn, J., Pittas, A. G., Slack, B. E., Growdon, J. H., and Wurtman, R. J. (1992) Evidence for a membrane defect in Alzheimer disease brain, *Proc. Natl. Acad. Sci. U.S.A. 89*, 1671−5.
46. Holmes-McNary, M. Q., Loy, R., Mar, M. H., Albright, C. D., and Zeisel, S. H. (1997) Apoptosis is induced by choline deficiency in fetal brain and in PC12 cells, *Brain Res. Dev. Brain Res. 101*, 9−16.
47. Suomensaari, S. M., Caccavello, R., Jacobson-Croak, K., Bales, C., Doan, M., Basi, G. S., Walker, D., Anderson, J. P., and Sinha, S. (2000) *Soc. Neurosci. Abstr. 26*, 1283.
48. Asami-Odaka, A., Ishibashi, Y., Kikuchi, T., Kitada, C., and Suzuki, N. (1995) Long amyloid β-protein secreted from wild-type human neuroblastoma IMR-32 cells, *Biochemistry 34*, 10272−8.
49. Wahrle, S., Das, P., Nyborg, A. C., McLendon, C., Shoji, M., Kawarabayashi, T., Younkin, L. H., Younkin, S. G., and Golde, T. E. (2002) Cholesterol-dependent γ-secretase activity in buoyant cholesterol-rich membrane microdomains, *Neurobiol Dis. 9*, 11−23.
50. Burns, M., Gaynor, K., Olm, V., Mercken, M., LaFrancois, J., Wang, L., Mathews, P. M., Noble, W., Matsuoka, Y., and Duff, K. (2003) Presenilin redistribution associated with aberrant cholesterol transport enhances β-amyloid production in vivo, *J. Neurosci. 23*, 5645−9.
51. Runz, H., Rietdorf, J., Tomic, I., de Bernard, M., Beyreuther, K., Pepperkok, R., and Hartmann, T. (2002) Inhibition of intracellular cholesterol transport alters presenilin localization and amyloid precursor protein processing in neuronal cells, *J. Neurosci. 22*, 1679−89.
52. Fassbender, K., Simons, M., Bergmann, C., Stroick, M., Lutjohann, D., Keller, P., Runz, H., Kuhl, S., Bertsch, T., von Bergmann, K., Hennerici, M., Beyreuther, K., and Hartmann, T. (2001) Simvastatin strongly reduces levels of Alzheimer's disease β-amyloid peptides Abeta 42 and Abeta 40 in vitro and in vivo, *Proc. Natl. Acad. Sci. U.S.A. 98*, 5856−61.
53. Simons, M., Keller, P., De Strooper, B., Beyreuther, K., Dotti, C. G., and Simons, K. (1998) Cholesterol depletion inhibits the generation of β-amyloid in hippocampal neurons, *Proc. Natl. Acad. Sci. U.S.A. 95*, 6460−4.
54. Fraering, P., Imhof, I., Meyer, U., Strub, J. M., van Dorsselaer, A., Vionnet, C., and Conzelmann, A. (2001) The GPI transamidase complex of *Saccharomyces cerevisiae* contains Gaa1p, Gpi8p, and Gpi16p, *Mol. Biol. Cell. 12*, 3295−306.
55. Tian, G., Sobotka-Briner, C., Zysk, J., Liu, X., Birr, C., Sylvester, M. A., Edwards, P. D., Scott, C. D., and Greenberg, B. D. (2002) Linear noncompetitive inhibition of solubilized human γ-secretase by pepstatin A methylester, L685458, sulfonamides, and benzodiazepines, *J. Biol. Chem. 277*, 31499−505.
56. Dovey, H. F., John, V., Anderson, J. P., Chen, L. Z., de Saint Andrieu, P., Fang, L. Y., Freedman, S. B., Folmer, B., Goldbach, E., Holsztynska, E. J., Hu, K. L., Johnson-Wood, K. L., Kennedy, S. L., Kholodenko, D., Knops, J. E., Latimer, L. H., Lee, M., Liao, Z., Lieberburg, I. M., Motter, R. N., Mutter, L. C., Nietz, J., Quinn, K. P., Sacchi, K. L., Seubert, P. A., Shopp, G. M., Thorsett, E. D., Tung, J., Wu, J., Yang, S., Yin, C. T., Schenk, D. B., May, P. C., Altstiel, L. D., Bender, M. H., Boggs, L. N., Britton, T. C., Clemens, J. C., Czilli, D. L., Dieckman-McGinty, D. K., Droste, J. J., Fuson, K., Gitter, B. D., Hyslop, P. A., Johnstone, E. M., Li, W. Y., Little, S. P., Mabry, T. E., Miller, F. D., and Audia, J. E. (2001) Functional γ-secretase inhibitors reduce β-amyloid peptide levels in brain, *J. Neurochem. 76*, 173−81.
57. Klafki, H., Abramowski, D., Swoboda, R., Paganetti, P. A., and Staufenbiel, M. (1996) The carboxyl termini of β-amyloid peptides 1-40 and 1-42 are generated by distinct γ-secretase activities, *J. Biol. Chem. 271*, 28655−9.
58. Wolfe, M. S., Xia, W., Moore, C. L., Leatherwood, D. D., Ostaszewski, B., Rahmati, T., Donkor, I. O., and Selkoe, D. J. (1999) Peptidomimetic probes and molecular modeling suggest that Alzheimer's γ-secretase is an intramembrane-cleaving aspartyl protease, *Biochemistry 38*, 4720−7.
59. Weggen, S., Eriksen, J., Das, P., Sagi, S. A., Wang, R., Pietrzik, C. U., Findlay, K. A., Smith, T. E., Murphy, M. P., Bulter, T., Kang, D., Marquez-Sterling, N., Golde, T. E., and Koo, E. H. (2001) A subset of NSAIDs lower amyloidogenic Abeta42 independently of cyclooxygenase activity, *Nature 414*, 212−6.
60. Takahashi, Y., Hayashi, I., Tominari, Y., Rikimaru, K., Morohashi, Y., Kan, T., Natsugari, H., Fukuyama, T., Tomita, T., and Iwatsubo, T. (2003) Sulindac sulfide is a noncompetitive γ-secre-

tase inhibitor that preferentially reduces Abeta 42 generation, *J. Biol. Chem. 278*, 18664−70.
61. Richardson, D. R., and Ponka, P. (1997) The molecular mechanisms of the metabolism and transport of iron in normal and neoplastic cells, *Biochim. Biophys. Acta 1331*, 1−40.
62. Xia, W., Zhang, J., Perez, R., Koo, E. H., and Selkoe, D. J. (1997) Interaction between amyloid precursor protein and presenilins in mammalian cells: implications for the pathogenesis of Alzheimer disease, *Proc. Natl. Acad. Sci. U.S.A. 94*, 8208−13.
63. Murphy, M. P., Uljon, S., Golde, T. E., and Wang, R. (2002) FAD-linked mutations in presenilin 1 alter the length of Abeta peptides derived from betaAPP transmembrane domain mutants, *Biochim. Biophys. Acta 1586*, 199−209.
64. Lichtenthaler, S. F., Beher, D., Grimm, H. S., Wang, R., Shearman, M. S., Masters, C. L., and Beyreuther, K. (2002) The intramembrane cleavage site of the amyloid precursor protein depends on the length of its transmembrane domain, *Proc. Natl. Acad. Sci. U.S.A. 99*, 1365−70.
65. Mammi, S., and Peggion, E. (1990) Conformational studies of human [15-2-aminohexanoic acid]little gastrin in sodium dodecyl sulfate micelles by ^{1}H NMR, *Biochemistry 29*, 5265−9.
66. Rizo, J., Blanco, F., Kobe, B., Bruch, M. D., and Gierasch, L. M. (1993) Conformational behavior of *Escherichia coli* OmpA signal peptides in membrane mimetic environments, *Biochemistry 32*, 4881−94.
67. Watanabe, Y. (2002) Effect of various mild surfactants on the reassembly of an oligomeric integral membrane protein OmpF porin, *J. Protein Chem. 21*, 169−75.
68. Kim, J. M., Booth, P., Allen, S. J., and Khorana, H. G. (2001) Structure and function in bacteriorhodopsin: the role of the interhelical loops in the folding and stability of bacteriorhodopsin, *J. Mol. Biol. 308*, 409−22.
69. Otzen, D. (2003) Folding of DsbB in mixed micelles: a kinetic analysis of the stability of a bacterial membrane protein, *J. Mol. Biol. 330*, 641−9.
70. Takasugi, N., Takahashi, Y., Morohashi, Y., Tomita, T., Iwatsubo, T. (2002) The mechanism of γ-secretase activities through high molecular weight complex formation of presenilins is conserved in *Drosophila melanogaster* and mammals, *J. Biol. Chem. 277*, 50198−205.

BI0494976